



Cite this: *Green Chem.*, 2021, **23**, 3502

## Microwave-assisted hydrothermal treatments for biomass valorisation: a critical review

Yang Gao, <sup>a</sup> Javier Remón <sup>b</sup> and Avtar S. Matharu <sup>\*a</sup>

The sustainable conversion of biomass into biofuels, chemicals and biomaterials has gained increasing attention to ensure the well-being of present and future generations. Among the different technologies available to date for the valorisation of biomass, microwave-assisted hydrothermal conversion has recently appeared as a state-of-the-art technology, capable of furnishing a wide range of reaction products for the energy, pharmaceutical and chemistry sectors. This emerging technology combines the inherent benefits of microwave heating and the sustainable features of biomass hydrothermal valorisation. Herein, for the first time, this critical review summarises and analyses all the work conducted to date on the use of microwave-assisted hydrothermal processes (including microwave-assisted carbonisation, liquefaction and treatment/hydrolysis) for the conversion of biomass into hydrochar, bio-crude (bio-oil) and valuable chemicals. In particular, this work has put together vital information addressing the influences of the reaction conditions (temperature, time, amount and type of catalyst, biomass loading and type, and microwave power) on the yields and key properties of the reaction products. The relationships between these processing parameters and the chemical transformations involved in the processes (hydrolysis, dehydration, decarboxylation, condensation and re-polymerisation) have been described in detail, and reliable comparisons have also been established between microwave-assisted and conventional hydrothermal technologies when data were available. As a result, this critical review collects essential information on the use of this cutting-edge, recently appeared microwave-assisted hydrothermal technology, and paves the way for its expansion and future development and commercialisation.

Received 17th February 2021

Accepted 6th April 2021

DOI: 10.1039/d1gc00623a

[rsc.li/greenchem](http://rsc.li/greenchem)

## 1. Introduction

The current global population (7.8 billion in 2020, which is expected to exceed over 10.9 billion by 2100<sup>1</sup>), along with the dramatic and continuous increase in industrialisation and urbanisation worldwide, brings an unprecedented and challenging scenario to satisfy the current and future consumption requirements with the finite resources available. However, the continued utilisation of non-renewable fossil resources is fraught with various environmental (e.g. pollution, and global warming) and social issues. As such, it is paramount to seek more sustainable and alternative approaches to cover the present and future chemical, material and energy needs.

Given this socio-economic scenario, biomass is seen as an ideal resource to obtain these commodities. In particular, lignocellulosic biomass, including agricultural and forestry residues, crops, wood, and urban wastes,<sup>2</sup> is one of the most abundant renewable resources on the Earth ( $1.0 \times 10^{11}$  tons

annually produced worldwide<sup>3</sup>). Besides, it is renewable, carbon-neutral and environmentally friendly. Structurally, biomass primarily consists of cellulose, hemicellulose and lignin, and its conversion allows furnishing a broad spectrum of biofuels, biomaterials and biochemicals.<sup>4–6</sup> Thus, using biomass as a feedstock minimises waste and pollution and offers a potentially sustainable alternative to replace crude oil to produce chemicals and energy. Regarding the latter, biomass is currently the world's fourth energy source (about 10–14%) after conventional fossil oil, coal and natural gas.<sup>4,7,8</sup> Therefore, knowing the finite nature of these fossil energy carriers, the International Energy Agency (IEA) estimates that almost half of the energy demand by 2050 should be produced from biomass.<sup>9</sup> Thus, over the past few decades, there has been a tremendous amount of work done in the area of biomass valorisation to produce valuable products (biochemicals and biomaterials) and energy (biofuels).<sup>2,10–12</sup>

Various technologies have been developed for biomass valorisation to achieve this goal, with biological and thermochemical processes being the two major conversion routes considered to date. Among these, thermochemical technologies are usually preferred over biological processes due to the shorter times used and the more beneficial economic costs

<sup>a</sup>Green Chemistry Centre of Excellence, University of York, Department of Chemistry, Heslington, York, YO10 5DD, UK. E-mail: [avtar.matharu@york.ac.uk](mailto:avtar.matharu@york.ac.uk)

<sup>b</sup>Instituto de Carboquímica, CSIC. C/Miguel Luesma Castán 4, 50018 Zaragoza, Spain



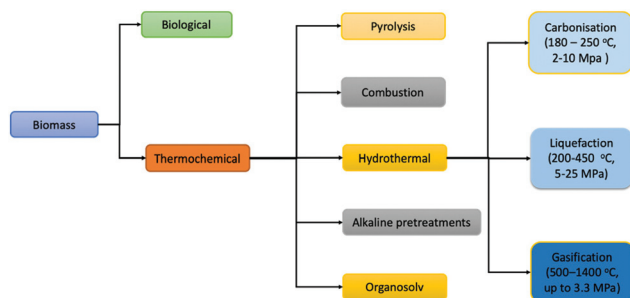


Fig. 1 Biomass conversion technologies. Adapted from Tekin.<sup>16</sup>

associated with the former technology.<sup>13</sup> Thermochemical procedures primarily include pyrolysis, gasification, combustion and hydrothermal treatments (Fig. 1).<sup>14,15</sup> Among these methods, hydrothermal processes are very advantageous to convert biomass into energy and/or high value-added products.<sup>16,17</sup> This technology uses hot liquid (subcritical or supercritical) water as the reaction medium to transform biomass into a pool of valuable products of different nature, including gases, liquids, and solids.<sup>18</sup>

Since the 1980s, when the Shell Oil Company applied this biomass conversion technology for the first time,<sup>16</sup> extensive work has been conducted on the hydrothermal treatment of biomass.<sup>18,19</sup> One of the main advantages of the hydrothermal treatment is that it uses water as the reaction medium. This dispenses with the need of using a high energy-consuming drying step and permits processing wet biomasses and slurries, which increases the energy efficiency of the process compared to classical methods such as pyrolysis and/or combustion. Besides, using water as a solvent provides other advantages, as it is clean, environmentally friendly, renewable, abundant and cheap.<sup>20</sup> Also, the hydrothermal treatment of biomass takes place at mild operation temperatures and uses moderate pressures, which reduces corrosion concerns and facilitates its scale-up and commercialisation.<sup>21–23</sup> As a result of these promising prospects, substantial work has been conducted on developing novel processes and new reactor designs and configurations to expand and develop this thermochemical process. In particular, the importance of process design, control and energy efficiency in the early-stage technology development was highlighted as critical to the economic and environmental viability of biomass hydrothermal conversion. The use of microwave heating, *i.e.*, converting electromagnetic radiation into heat energy within the target material, has been recently considered one of the most promising technologies to replace conventional heating during the valorisation of biomass.<sup>24–31</sup>

## 2. Microwave-assisted hydrothermal technology

Based on the dipole rotation of polar molecules and ionic conduction with high frequency (300 MHz to 300 GHz), microwave

radiation transforms the electromagnetic energy directly into heat energy, resulting in fast and selective heating of the reaction medium and the biomass material under consideration.<sup>32,33</sup> Since 1986, when Gedye *et al.*<sup>34</sup> reported the term ‘microwave-assisted’ synthesis for the first time, extensive work has been conducted on biomass conversion *via* microwave-assisted processes. These include chemical synthesis, digestion, extraction, drying, cooking, and pyrolysis.<sup>35–39</sup> Compared to traditional heating, microwave-assisted heating has several benefits for the conversion of biomass. These include being (i) volumetric and uniform at the molecular level, allowing rapid and direct heating of the target material, which in some cases can save time and energy, thus improving the conversion efficiency;<sup>40</sup> (ii) controllable, which leads to higher yields and reduces reaction times;<sup>41</sup> and (iii) more selective, reducing the amounts of side-products.<sup>42</sup>

Given these inherent benefits of microwave heating, and bearing in mind that water is highly effective in microwave energy absorption, achieving hydrothermal conditions through microwave heating to conduct hydrothermal reactions has recently arisen as a promising technology for biomass valorisation. On the one hand, water has good microwave energy absorption properties from a microwave-assisted perspective due to its high dielectric constant ( $\delta'$ ) and loss tangent ( $\tan \delta$ ). On the other hand, from a hydrothermal viewpoint, water behaves as both the reaction medium and the catalyst. Concerning the former, water under subcritical (100–374 °C) or supercritical (above 374 °C and pressure above 22.1 MPa) conditions has excellent solubilisation capability to dissolve organic compounds, which facilitates biomass conversion.<sup>20,43–45</sup> Regarding the latter, water has a high ionic product, promoting acid- and/or base-catalysed reactions (*e.g.* hydrolysis). Simultaneously, the high density and elevated dissociation constant of water under hydrothermal conditions also accelerate ionic reactions (*e.g.* dehydration), thus converting water into an excellent reaction medium for the hydrothermal conversion of biomass.<sup>46,47</sup> Given all these factors, the combination of hydrothermal conditions together with microwave-assisted heating, *i.e.*, ‘microwave-assisted hydrothermal treatment’, has recently been regarded as a novel, up-and-coming and efficient technology to achieve a selective and controllable biomass conversion.<sup>41</sup>

Although there are some review publications in the literature addressing the use of microwave-assisted heating for biomass conversion,<sup>33,48</sup> the use of microwave technology to conduct hydrothermal reactions was not considered, as these reviews focused on microwave-assisted pyrolysis and torrefaction. As such, to the best of the author’s knowledge, the use of microwave-assisted hydrothermal treatments for biomass valorisation has not yet been reviewed. Herein, this work summarises and critically analyses the current state of the art on the use of microwave-assisted hydrothermal treatments, including microwave-assisted hydrothermal liquefaction (MA-HTL), carbonisation (MA-HTC) and treatment/hydrolysis (MA-HTT), for the conversion of biomass into liquid and solid biofuels and value-added chemicals (Fig. 2). A comparison



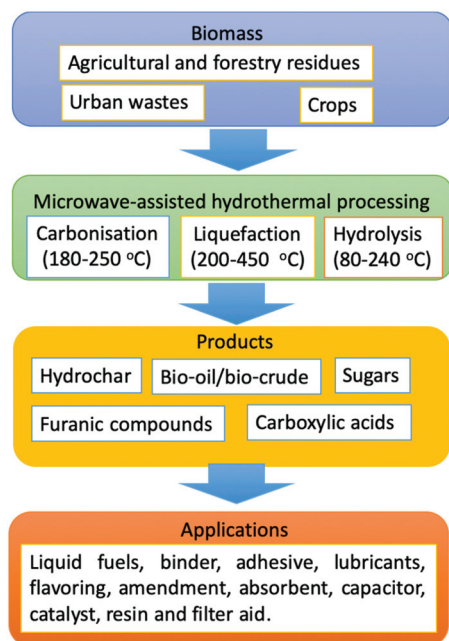


Fig. 2 Conceptual biorefinery via the microwave-assisted hydrothermal treatment of biomass.

between hydrothermal carbonisation, liquefaction and treatment/hydrolysis is listed in Table 1. In particular, this critical review brings together, analyses and discusses the recent research progress achieved to date in the microwave-assisted hydrothermal valorisation of biomass from a biorefinery perspective. This includes the effects of the type of biomass (feedstock), operating conditions (temperature, time, pressure) and catalyst type and loading on the overall distribution of the reaction products (yields) and fundamental fuels and the physicochemical properties of these fractions. Given the lack of work covering and comparing all the research conducted in this field, this review provides an excellent overview to expand and develop this emerging technology.

### 3. Microwave-assisted hydrothermal carbonisation (MA-HTC)

Microwave-assisted hydrothermal carbonisation (MA-HTC) has recently received a lot of attention due to its several advantages

for biomass conversion. These include high conversion efficiency, low processing temperatures, and the capability to process wet and aqueous feedstocks.<sup>49–51</sup> During the MA-HTC process, biomass is subjected to moderate temperatures (180–250 °C) and pressures (2–10 MPa, usually autogenous) for a short reaction time (dozens of minutes to a few hours).<sup>52,53</sup> During this process, several chemical reactions, such as dehydration, decarboxylation, hydrolysis, polymerisation, polycondensation, and aromatisation, take place.<sup>54</sup> As a result of these transformations, the relative amounts of hydrogen and oxygen in the material decrease. At the same time, the proportion of C and the HHV increase, which leads to the production of an energy-dense and carbon-rich solid material, known as hydrochar.<sup>55</sup>

Hydrochar produced from biomass has several beneficial properties, such as a high energy density, high carbon content, high mechanical strength, and non-fibrous structure.<sup>56,57</sup> Therefore, it can be used in multiple potential applications, including amendments, absorbents, capacitors, fuels, catalysts, and filter aids.<sup>58–61</sup> Compared to conventional hydrothermal carbonisation, MA-HTC is faster, more controllable and friendly and energy and technologically more efficient. As a result of these features, a substantial amount of work has been conducted on using this technology to convert biomass into hydrochar to be used for energy production and material applications (Table 2).

#### 3.1 Effect of the operating conditions during the MA-HTC of biomass

The yield and fuel and physicochemical properties of the hydrochar produced during the MA-HTC of biomass primarily depend on the reaction temperature, time, catalyst (type and amount) and solid/liquid ratio. Besides, other factors such as the biomass type, microwave power and particle size also exert a significant, but less critical influence. The effects of these variables are summarised as follows.

**3.1.1 Reaction temperature.** Reaction temperature plays one of the most influential roles in the MA-HTC process.<sup>62</sup> In particular, it significantly directs the distribution of the main reaction products (gas, liquid or bio-crude and solid or hydrochar) and determines the primary fuel and physicochemical properties of these fractions. In the scope of this section, the influence of the reaction temperature is only discussed on the yields and properties of the hydrochar.

Table 1 Comparison between hydrothermal carbonisation, liquefaction and hydrolysis/treatment

Method	Temp. (°C)	Pressure (MPa)	Biomass loading	Catalyst	Products
Hydrothermal carbonisation	180–250	2–10	1 : 1–1 : 30	Acids, alkalis	Hydrochar (a source for solid biofuels and biomaterials)
Hydrothermal liquefaction	200–450	5–25	1 : 4–1 : 50	Acids, alkali salts, metal oxides, zeolites and carbon nanotubes	Bio-crude/bio-oil (a source for liquid biofuel and chemicals)
Hydrothermal treatment/hydrolysis	80–240	—	1 : 1–1 : 40	Acids, carbon, transition metal chlorides	Value-added chemicals: sugars, furans and carboxylic acids



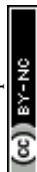
Table 2 Summary of the literature on the microwave-assisted hydrothermal carbonisation of biomass

Biomass	Reaction parameters	Catalyst	Application	Reference
Rice straw	Temperature (160–200 °C), time (40–70 min), solid/liquid ratio (1 : 10)	—	Adsorbent	Li <i>et al.</i> <sup>76</sup>
Pig faeces	Temperature (150–250 °C), time (0–120 min), solid/liquid ratio (0.01–0.2 g ml <sup>-1</sup> )	CaO, H <sub>2</sub> SO <sub>4</sub>	Adsorbent	Wang <i>et al.</i> <sup>65</sup>
Human biowastes	Temperature (160–200 °C), time (30–120 min), solid/liquid ratio (1 : 10)	—	Fuel resource	Afolabi <i>et al.</i> <sup>56</sup>
Corn stalk	Temperature (122.7–257.3 °C), time ((4.8–55.2 min), solid/liquid ratio (0.98–6.02 g per 50 mL H <sub>2</sub> O)	—	Solid biofuel	Kang <i>et al.</i> <sup>66</sup>
Dairy manure	Temperature (180–260 °C), time (30 min–14 h), solid/liquid ratio (1 : 20)	—	Carbon-based nanomaterials	Gao <i>et al.</i> <sup>72</sup>
Rapeseed husk	Temperature (150–200 °C), time (2–30 min), solid/liquid ratio (1 : 15)	—	Solid fuel	Elaigwu <i>et al.</i> <sup>78</sup>
Pine sawdust, α-cellulose	Temperature (200 °C), time (60–240 min), solid/liquid ratio (1 : 20)	Citric acid	Energy and materials	Gutoku <i>et al.</i> <sup>79</sup>
Fish waste	Temperature (150–210 °C), time (90–120 min)	—	Energy applications	Kannan <i>et al.</i> <sup>73</sup>
Green waste	Temperature (130–190 °C), time (0.5–2 h), solid/liquid ratio (1 : 7–1 : 10)	—	Fuel resource	Shao <i>et al.</i> <sup>67</sup>
Rice husk	Temperature (160–220 °C), time (30 min), solid/liquid ratio (1 : 1)	—	Fuel resource	Nizamuddin <i>et al.</i> <sup>68</sup>
Coconut shell	Temperature (150–200 °C), time (5–30 min), solid/liquid ratio (1 : 15)	—	Renewable fuels	Elaigwu <i>et al.</i> <sup>75</sup>
Phoenix tree leaves	Temperature (220–260 °C), time (30–90 min), solid/liquid ratio (1 : 30)	HCl/NaOH	Energy and materials	Xu <i>et al.</i> <sup>69</sup>
Grapefruit peel	Temperature (213 ± 2 °C), time (20 min), solid/liquid ratio (1 : 3 (w/v))	—	Adsorbent	Semeriz <i>et al.</i> <sup>61</sup>
Red seaweed	Temperature (160–200 °C), time (1–40 min), solid/liquid ratio (1%–10%, w/v)	H <sub>2</sub> SO <sub>4</sub>	Solid fuel	Cao <i>et al.</i> <sup>80</sup>
Sugarcane bagasse	Temperature (180 °C), time (5, 15, 30 min), solid/liquid ratio (1 : 5, 1 : 10)	H <sub>2</sub> SO <sub>4</sub>	Solid fuels	Chen <i>et al.</i> <sup>81</sup>
Furfural residue	Temperature (200 °C), time (30 min), solid/liquid ratio (1 : 7)	—	Adsorbent	Khushk <i>et al.</i> <sup>71</sup>
Fruit waste	Temperature (200 °C), time (120 min), solid/liquid ratio (1 : 20)	Citric acid	Methane storage	Cruz Jr <i>et al.</i> <sup>60</sup>
Red macroalgae Eucheuma denticulatum	Temperature (150–170 °C), time (10 min), solid/liquid ratio (1 : 20)	H <sub>2</sub> SO <sub>4</sub>	Energy and materials	Teh <i>et al.</i> <sup>82</sup>
Bamboo sawdust	Temperature (150–230 °C), time (5–35 min), solid/liquid ratio (1 : 10)	—	Biofuel	Bundhoo <i>et al.</i> <sup>53</sup>
Willow wood	Temperature (150–185 °C), time (60 min), solid/liquid ratio (1 : 20)	—	Solid fuel	Knapp <i>et al.</i> <sup>83</sup>
<i>Prosopis africana</i> shell	Temperature (200 °C), time (5–20 min), solid/liquid ratio (1 : 15)	—	Energy and materials	Elaigwu <i>et al.</i> <sup>84</sup>
Lincomycin residue	Temperature (120–210 °C), time (60 min), solid/liquid ratio (1 : 10)	—	Adsorbent	Ahmad <i>et al.</i> <sup>85</sup>

Generally, higher temperatures provide more energy to break down the chemical bonds within the biomass structural components (mainly cellulose, hemicellulose and lignin), which also leads to a more significant spread of liquefaction and gasification reactions. These transformations promote the formation of more liquid (bio-crude) and gaseous products, which leads to opposing effects. On the one hand, these reactions decrease the amounts of oxygen and hydrogen in the hydrochar. Still, on the other hand, they also decrease the hydrochar yield.<sup>52,63</sup> As a result of these developments, the hydrochar yield is high at relatively low temperatures. It decreases with increasing temperature, while the physico-chemical properties of this solid are enhanced as the temperature increases.

Given these opposing influences, the specific effects of the temperature on the yield and properties of the hydrochar have been addressed by several authors. However, different outcomes were observed due to the diverse chemical compositions of the feedstocks used and the ample ranges of temperatures applied. For example, Nizamuddin *et al.*<sup>64</sup> concluded that the hydrochar yield decreased continuously (from 58.6 to 49.5%) with rising temperature from 160 to 220 °C during the MA-HTC of rice husk, which is in line with the trends reported in the literature.<sup>56,65–71</sup> In contrast, Gao *et al.*<sup>72,73</sup> demonstrated that the hydrochar yield produced during the MA-HTC of fish waste firstly increased with increased temperature. It then reached a point after which it decreased with further temperature increments. These differences may be accounted for by the different chemical compositions of the feedstocks under consideration (dairy manure vs. fish waste), thus highlighting the influence of the biomass composition on the process. In particular, Elaigwu *et al.*<sup>74,75</sup> reported a first increment in the hydrochar yield followed by a subsequent decline during the MA-HTC of lignocellulosic feedstocks. They concluded that the first increase might result from side reactions occurring between some lignin-derived volatile compounds and hemicellulose carbonised species, which overall increased the amount of solid matter, thus increasing the hydrochar yield. As an exception to these trends, Li *et al.*<sup>76</sup> showed that increasing the temperature between 160 and 200 °C did not significantly impact the hydrochar yield during the MA-HTC of rice straw. Also, it must be borne in mind that higher temperatures may result in different outcomes for the hydrochar yield than those described above. For example, Liu *et al.*<sup>77</sup> reported that when temperatures higher than 200 °C were used, the hydrochar yield increased with the temperature, probably due to the positive effect of the temperature on repolymerisation, condensation and crystallisation reactions. Thus, these results indicate that the optimum temperature to strike a good balance between the yield and the properties of the hydrochar depends on the biomass nature and processing conditions, and therefore it must be determined experimentally. Considering the information shown above, this temperature might shift between 180 and 250 °C.

**3.1.2 Reaction time.** In general, prolonging the reaction time increases the carbonisation of biomass and promotes the



formation of lighter organic compounds and/or gases,<sup>86</sup> which consequently drops the hydrochar yield. However, an increase in the reaction time also favours the development of condensation and repolymerisation reactions, which leads to an increase in the production of hydrochar. Several authors have addressed the detailed influence of this variable during the MA-HTC of different types of biomass. Jacobson *et al.*<sup>87</sup> reported that after a first decrease in the hydrochar yield with the increase in the reaction time, the hydrochar yield reached a trend-off with time due to the almost complete decomposition of the cellulose and hemicellulose contents in the biomass. Wang *et al.*<sup>65</sup> investigated the MA-HTC of pig faeces at 230 °C, using a solid/water ratio of 0.05 g biomass per mL water. They reported that the yield of hydrochar decreased very sharply (from 61.1 to 55.7%) within the first 120 min of microwave treatment, and then the decline observed was less pronounced. This development was also reported by Elaigwu *et al.*,<sup>78</sup> who found that the hydrochar yield substantially decreased within the first minutes of the reaction. In particular, around 14% of mass loss took place during the first 20 min of operation, while it remained stable with a further increase in the reaction time.

In contrast, Guiotoku *et al.*<sup>74</sup> found a different trend during the MA-HTC of pine sawdust in an acidic aqueous medium at 200 °C. They reported that the hydrochar yield increased with prolonging the reaction time and indicated that such an increase might be accounted for by the deposition of volatile compounds on the surface of the material. Besides, other authors have also found a steady time evolution for the hydrochar yield.<sup>72</sup> These different developments demonstrate significant interactions between the biomass chemical composition and the reaction time, which suggests that the particular influence of the reaction time must be assessed for each type of biomass under consideration. Therefore, the optimum reaction time must be determined experimentally; however, considering the results shown above, the optimum reaction time might be between 20 and 60 min.

**3.1.3 Catalyst.** The catalyst (type and loading) exerts a substantial influence on the MA-HTC of biomass. In particular, the presence of a catalyst in the reaction medium promotes the depolymerisation of biomass and the formation of hydrochar during the MA-HTC process. However, publications considering the use of a catalyst for the MA-HTC of biomass are very scarce.<sup>88</sup> Consequently, the impacts of using a catalyst on the hydrochar yield and properties are not yet well understood. Wang *et al.*<sup>65</sup> used H<sub>2</sub>SO<sub>4</sub> as a catalyst in the MA-HTC of pig faeces and found that the hydrochar yield decreased from 60 to 49 wt% when the process was conducted with a catalyst. They reported that the catalyst boosted biomass hydrolysis reactions, increasing the biomass transformation into gas and liquid species and decreasing the hydrochar yield. Contrariwise, when CaO catalysed the MA-HTC process, the solid yield increased from 60 to 66 wt%. However, they believed that such an increased yield could have been accounted for by forming solid CaCO<sub>3</sub> from CaO, thus contributing to the global production of solid matter.

**3.1.4 Other factors: solid to water ratio, microwave power and biomass particle size.** Generally, as microwave energy is limited by the penetration depth, a high solid/water ratio would restrict the microwave irradiation to break down the polymeric biomass structure.<sup>66</sup>

Thus, the greater the solid/water ratio, the higher is the hydrochar yield produced during the MA-HTC of biomass. While most of the biomasses can be processed by HTT due to their hydrophilic nature and reasonable capability to form pumpable slurries, the solid/water ratio must be adjusted experimentally. In general, it shifts between 5 and 50 wt%; however, the maximum ratio must be determined experimentally depending on the biomass nature and the type of reactor (batch/continuous). An increase in the solid amount logically decreases the amount of water available to ensure an efficient penetration. Consequently, the hydrothermal carbonisation is not complete, which increases the yield of hydrochar.<sup>53,66</sup> Several authors have analysed the effect of this factor. Wang *et al.*<sup>65</sup> reported that increasing the solid/liquid ratio from 0.01 g mL<sup>-1</sup> to 0.2 g mL<sup>-1</sup> led to an increase in the hydrochar yield from 51 to 69% during the MA-HTC of pig faeces at 230 °C for 30 min. Nizamuddin *et al.*<sup>68</sup> also evidenced an increase (from 47 to 51%) in the hydrochar yield with increasing the biomass loading (from 1 : 40 w/v to 1 : 10 w/v). However, the effect of the solid/water ratio can also depend on the other processing conditions. For example, Kannan *et al.*<sup>73</sup> reported that an increase in the biomass/water ratio from 0.5 to 1.5 wt% did not significantly influence the hydrochar yield when the process was conducted at 180 °C for 60 min.

The type and structural composition of the biomass also affect the hydrochar yield. Cellulose and hemicellulose, being polysaccharides, are easily degraded into gas and liquid species during the MA-HTC process. In contrast, lignin quickly evolves towards the formation of hydrochar due to its inherent compact and poly-aromatic structure.<sup>52</sup> Thus, the more significant the proportion of lignin within the biomass, the higher is the hydrochar yield. However, the specific effect of the biomass composition on the hydrochar yield has not been substantially addressed in the literature. Some studies include the work of Afolabi *et al.*,<sup>56</sup> who investigated the MA-HTC of human biowastes and found that the type and nature of the feedstock affected the hydrochar yield. In another study, Kang *et al.*<sup>89</sup> reported the hydrochar yield obtained during the MA-HTC of various feedstocks, and found that it decreased as follows: lignin > wood meal > cellulose > D-xylose. These results are in good agreement with the reaction mechanism describing the decomposition of biomass when subjected to hydrothermal conditions. On the one hand, a higher hydrochar yield was produced during the MA-HTC of lignin, due to the stable phenolic structure of this structural compound. On the other hand, the lowest hydrochar yield was obtained during the treatment of D-xylose, due to its labile structure, which can easily evolve towards the formation of gaseous and liquid species.<sup>69,90</sup>

The microwave irradiation power and the biomass particle size also significantly influence the hydrochar yield, although



their impacts are less significant from a practical point of view. In particular, increasing the microwave power favours the development of biomass depolymerisation side reactions, such as volatilisation and decomposition, which overall decreases the hydrochar yield.<sup>91,92</sup> Nizamuddin *et al.*<sup>64</sup> studied the effect of the biomass particle size (1–3 mm) during the MA-HTC of rice straw. They reported that an increase in the biomass particle size promoted the formation of hydrochar due to the decrease occurring in the surface of biomass surrounded by water and efficiently exposed to microwave radiation.

### 3.2 Hydrochar fuel and physicochemical properties

**3.2.1 Higher heating value (HHV).** The Higher Heating Value (HHV) is one of the essential properties of hydrochar for evaluation of its potential application as a solid biofuel.<sup>93</sup> Usually, the higher the proportion of carbon in the material and the lower the ash, moisture and oxygen contents, the greater is the HHV of the hydrochar. The influence of the MA-HTC processing conditions on the HHV of the hydrochar has been assessed by several authors, who concluded that both the reaction conditions and the biomass type significantly influence the HHV of hydrochar. Shao *et al.*<sup>67</sup> revealed that an increase in the MA-HTC process parameters (temperature and time) facilitated the production of hydrochar with a higher HHV. In particular, increasing the temperature (from 160 to 190 °C) increased the HHV of the hydrochar from 17.91 to 23.01 MJ kg<sup>-1</sup> with 1 h holding time and 1 : 8 m/m biomass loading. Also, increasing the reaction time (from 0.5 to 1 h) increased the HHV from 21.95 to 23.01 MJ kg<sup>-1</sup> at 190 °C and 1 : 9 m/m solid/liquid ratio. Chen *et al.*<sup>81</sup> also reported the same developments.

Besides, the catalyst loading and the solid/water ratio also play crucial roles in the HHV of hydrochar. Regarding the former, Cao *et al.*<sup>80</sup> reported that an increment in the amount of catalyst from 0 to 0.6 H<sub>2</sub>SO<sub>4</sub> M led to increases in both the C content (from 45.6 to 55.9%) of the hydrochar and its HHV (from 17.9 to 23.3 MJ kg<sup>-1</sup>). Concerning the latter, Shao *et al.*<sup>67</sup> found that different HHVs (between 21.49 and 23.01 MJ kg<sup>-1</sup>) were obtained during the MA-HTC of biomass, depending on the solid/liquid ratio (1 : 8–1 : 9 m/m). In another study, Cao *et al.*<sup>80</sup> reported that when the MA-HTC was conducted at 180 °C for 20 min with 0.2 M H<sub>2</sub>SO<sub>4</sub> as a catalyst, an increase in the biomass loading from 1 to 5 wt% led to increases in the C content (from 53.8 to 56%), HHV (from 21.5 to 23.7 MJ kg<sup>-1</sup>) and EDs (from 1.72 to 1.89) of the hydrochar. However, a further increase in the biomass loading up to 10 wt% decreased the HHV (20.5 MJ kg<sup>-1</sup>) and ED (1.64).

The heating mechanism also significantly impacts the HHV of the hydrochar produced by MA-HTC of biomass. Dai *et al.*<sup>94</sup> established a comparison between the HHV of hydrochar produced using conventional HTT and MA-HTT. They found that the HHVs of the hydrochar produced using microwave technology were higher than their counterparts obtained by traditional heating. Such a difference was believed to be accounted for by a hot spot effect occurring with microwave heating, which promoted the rupture of low energy C–H and

C–O bonds, thus highlighting the benefits of microwave irradiation in the valorisation of biomass into energy-dense hydrochar.

A summary of the HHVs (MJ kg<sup>-1</sup>) of the hydrochar produced by MA-HTC of various biomasses is provided in Table 2.

**3.2.2 Elemental composition.** The ultimate analysis of hydrochar provides essential insights into not only the characterisation of these solids, but also the reaction mechanism of the MA-HTC process.<sup>57</sup> The reactions involved primarily include deoxygenation, dehydration, and decarboxylation, which overall decrease the amounts of hydrogen and oxygen in the hydrochar.<sup>78,81</sup> At the same time, the carbon content of the hydrochar increases due to condensation and aromatisation reactions.<sup>84</sup> The spread of these reactions can be gathered from the Van Krevelen diagram, representing the atomic H/C and O/C ratios of the biomass/hydrochar.<sup>95</sup> The O/C ratio describes the polarity, and the higher this ratio is, the more polar functional groups are available in the material. Similarly, the H/C ratio indicates the aromaticity of the hydrochar.<sup>95</sup> As such, the spread of the main types of reactions, *i.e.*, dehydration, decarboxylation, and demethylation, occurring during the MA-HTC is determined *via* the length of the vector drawn from the raw material to the hydrochar under consideration (Fig. 3).<sup>69</sup> The effects of the processing conditions on the elemental composition of the hydrochar produced by MA-HTC of biomass have been analysed by several authors. The elemental compositions of different hydrochars are summarised in Table 3.

**3.2.3 Fourier transform infrared (FTIR) spectroscopy.** FTIR spectra provide insights into some of the chemical changes occurring during the MA-HTC. These chemical transformations affect various hydrochar properties (*e.g.* pH, biodegradability, and hydrophobicity), thus significantly influencing the potential future applications of this material.<sup>66</sup> The typical bands observed during the FTIR analysis of hydrochar are listed in Table 4. As a result of the chemical transformations taking place during the HTC of biomass, this analysis shows decreases and increases in the signals of several bands. These

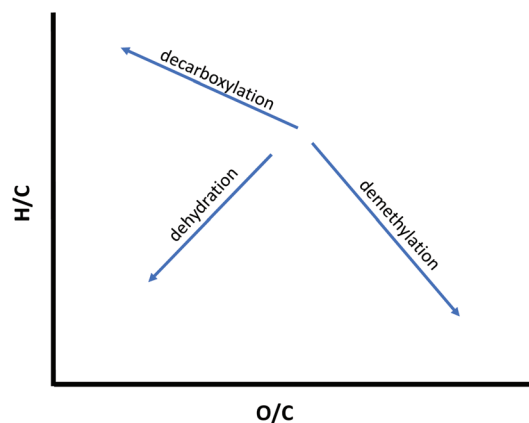


Fig. 3 Van Krevelen diagram for reaction pathways during the microwave-assisted hydrothermal processing of biomass.



**Table 3** Elemental Composition (wt%) and HHV (MJ kg<sup>-1</sup>) of the hydrochar produced from the MA-HTC of various biomasses

Hydrochar source	Elemental composition					HHV (MJ kg <sup>-1</sup> )	Hydrochar yield (%)	Reference
	C (wt%)	H (wt%)	N (wt%)	S (wt%)	O (wt%)			
Rice straw	37.44–42.74	3.18–5.72	0.40–1.15	0.04–0.35	30.73–40.76	—	37.00–42.53	Li <i>et al.</i> <sup>76</sup>
Rice straw	48.8	5	0.4	0.5	45.3	17.8	—	Nizamuddin <i>et al.</i> <sup>64</sup>
Pig faeces	52.2–56.6	4.21–7.40	2.35–3.66	—	35.4–37.3	21.5–23.4	24.6–65.6	Wang <i>et al.</i> <sup>65</sup>
Corn stock	45.89–53.44	5.67–5.85	1.00–1.14	—	39.64–47.07 <sup>a</sup>	22.82 <sup>b</sup>	73.94 <sup>b</sup>	Kang <i>et al.</i> <sup>66</sup>
Rapeseed husk	44.13–54.62	6.32–6.61	5.84–6.74	—	33.52–43.09 <sup>a</sup>	21.57 <sup>b</sup>	Around 42.5–63.5	Elaigwu <i>et al.</i> <sup>78</sup>
Red seaweed	48.8–57.8	5.4–6.0	1.0–1.9	—	35.2–44.0 <sup>a</sup>	18.8–24.7	20.8–31.4	Cao <i>et al.</i> <sup>80</sup>
Red macroalgae	48.10–56.18	5.85–6.37	1.12–1.95	—	36.53–43.58 <sup>a</sup>	14.93–18.07	20.54–31.77	Teh <i>et al.</i> <sup>82</sup>
Green waste	—	—	—	—	—	17.91–23.01	50.4–76.8	Shao <i>et al.</i> <sup>67</sup>
Palm kernel shell	69.20	3.30	0.61	0.04	—	27.63	—	Zainal <i>et al.</i> <sup>96</sup>
Sugarcane bagasse	44.48–52.35	4.34–5.43	0.25–0.38	0	36.82–48.88	18.45–20.58	39.6–70.4	Chen <i>et al.</i> <sup>81</sup>
	36.6–39.5	4.9–5.95	3.14–7.76	0.67–0.84	26.7–34.1 <sup>c</sup>	—	44.8–93.3	
Bamboo sawdust	48.15–50.14	5.53–5.65	<0.30	—	41.13–43.90	18.27–20.83	About 84–97	Dai <i>et al.</i> <sup>70</sup>
<i>Prosopis africana</i> shell	55.46–58.08	6.18–6.71	1.48–1.61	—	34.13–36.35	21.84–22.37	30.60–36.37	Elaigwu <i>et al.</i> <sup>84</sup>

<sup>a</sup> Oxygen was calculated by difference (100% – (C% + H% + N%)). <sup>b</sup> The data obtained are maximum values. <sup>c</sup> Oxygen was calculated by difference (100% – (C% + H% + N% + S%)).

**Table 4** Major band assignments in the FTIR analysis of hydrochar

Absorption band (cm <sup>-1</sup> )	Assignment	Component	Reference
3400–3200	O–H stretching vibration	Hydroxyl or carboxyl groups	Bundhoo <i>et al.</i> <sup>53</sup>
3000–2800	C–H stretching vibration	Aliphatic methylene group	Afolabi <i>et al.</i> <sup>56</sup>
1800–1600	C=O stretching vibration	Esters, carboxylic acids or aldehydes in cellulose	Elaigwu <i>et al.</i> <sup>78</sup>
1743	C=O stretching	Carbonyl, esters or carboxyl	Afolabi <i>et al.</i> <sup>56</sup>
1730	C=O	Carboxylic acid groups in hemicellulose	Semerçioz <i>et al.</i> <sup>61</sup>
1700	C=O	Ketones, aldehydes, and carboxylic acids	Semerçioz <i>et al.</i> <sup>61</sup>
1630	C=O	Carboxyl group in an aromatic ring	Teh <i>et al.</i> <sup>82</sup>
1600–1500	C=C vibrations	Aromatic ring in lignin	Li <i>et al.</i> <sup>67,76</sup>
1470–1430	C–H stretching	Methoxy	Gao <i>et al.</i> <sup>72</sup>
1450–1200	C–H bending vibration	Methylene, and methyl groups in aliphatic carbons	Elaigwu <i>et al.</i> <sup>78</sup>
1440–1400	O–H	Acids	Gao <i>et al.</i> <sup>72</sup>
1417	C–H vibrations	Aromatic	Nizamuddin <i>et al.</i> <sup>64</sup>
1367	O–H	Aromatic bend	Afolabi <i>et al.</i> <sup>56</sup>
1321	C–N stretching vibration	Aromatic structure	Shao <i>et al.</i> <sup>67</sup>
1324	C–H vibration or C–O vibration	Cellulose or syringyl derivatives	
1200–1000	C–O	Esters, phenols and aliphatic alcohols	Elaigwu <i>et al.</i> <sup>78</sup>
1241	C–O stretching or C–O–C stretching	Lignin or cellulose	Shao <i>et al.</i> <sup>61,67</sup>
1050	C–O–C	Polysaccharide bands	Afolabi <i>et al.</i> <sup>97</sup>
880–700	C–H vibrations	Aromatic structure	Afolabi <i>et al.</i> <sup>56</sup>
777, 650	C–H vibrations	Aromatic structure	Shao <i>et al.</i> <sup>67</sup>

predominantly include variations in the bands referring to the biomass structural components, such as cellulose/hemicellulose decreases, especially at high processing temperatures (*e.g.* 3400–3200 cm<sup>-1</sup> to polysaccharide and 1730 cm<sup>-1</sup> to hemicellulose). They are also responsible for new bands related to carbonised species developed during the process (1700 cm<sup>-1</sup>, 880–700 cm<sup>-1</sup>).<sup>97</sup> Work conducted on the FTIR analysis of hydrochar produced by MA-HTC of biomass is very scarce. Gao *et al.*<sup>72</sup> reported that the hydrochar produced by MA-HTC of biomass had better chemical functional features compared to those of the hydrochar produced by conventional heating.

**3.2.4 Thermogravimetric analysis.** The thermogravimetric decomposition analysis of biomass and related materials, such

as hydrochar, provides valuable information on their thermal stability and can be used to determine their fibre composition. This composition includes the moisture and volatile contents along with the proportions of cellulose, hemicellulose and lignin in the material. In this regard, the thermal decomposition of lignocellulosic biomass and derived hydrochar can be divided into three major stages: (i) the removal of moisture content and volatile compounds (below 120 °C); (ii) the decomposition of hemicellulose and cellulose (220–400 °C); and (iii) the deterioration of lignin and/or non-volatile matter with high thermal stability (above 400 °C).<sup>64,66,78</sup> Some authors have analysed the progressive decomposition of biomass occurring during the MA-HTC by thermogravimetric analysis using this information. It was found that the use of high temp-



eratures and/or long reaction times produced a progressive decrease in the hemicellulose peak until it completely disappeared. At the same time, the peak referring to the cellulose content moved towards higher temperatures, which revealed an increase in the thermal stability of cellulose during the process.<sup>70</sup> This was believed to be a consequence of the depletion of amorphous regions of cellulose fibrils and retention of highly compact crystalline cellulose, which increased the decomposition temperature of this fraction.<sup>98</sup> This information was in good agreement with the work of Dai *et al.*,<sup>94</sup> who used this analysis to compare the thermal stability of hydrochar produced by conventional HTC and MA-HTC. They found that the hydrochar produced with the former technology was more thermally stable than that obtained by microwave heating.

**3.2.5 Scanning electron microscopy (SEM) and Brunauer–Emmett–Teller (BET) characterisation.** SEM analysis has been used to study and discuss the changes occurring in the morphological structures of biomass and hydrochar during HTC. In particular, the characterisation of the hydrochar and original feedstocks revealed that the hydrochar usually had rougher and more disoriented surface features compared to the raw materials from which they were produced.<sup>66</sup> These developments are accounted for by a series of decomposition reactions experienced by the most abundant biomass structural components (cellulose, hemicellulose, and part of lignin) during the treatment. The most significant transformations include the hydrolysis and dehydration of polysaccharides, which develop microspheres on the surface of the hydrochar to minimise the energy interface.<sup>74</sup>

The effects of the MA-HTC processing conditions on the surface properties of hydrochar have been analysed by some authors. For example, Shao *et al.*<sup>67</sup> reported that increasing the temperature (130–190 °C) and/or extending the holding time (0.5–2 h) not only augmented the number of pores on the surface of hydrochar, but also reduced the formation of microspheres. In contrast, these authors also reported that an increase in the solid/liquid ratio (between 1 : 7–1 : 10 m/m) did not significantly impact the surface features of hydrochar. In another study, Gao *et al.*<sup>72</sup> found that extending the reaction time led to complete cellulose and hemicellulose decompositions and increased the number of microspheres. In this line, Elaigwu *et al.*<sup>78</sup> also observed the presence of cumulated, sphere-like microparticles (1–10 µm) formed from cellulose decomposition and demonstrated (Fig. 4) that the partial degradation of lignin was responsible for the rough texture of hydrochar.<sup>42,72,78</sup>

The development of a fine porous structure is paramount for the potential application of hydrochar as an advanced biomaterial, as reported by Nizamuddin *et al.*<sup>64</sup> These authors pointed out that the hydrochar produced by the MA-HTC of rice straw under optimum processing conditions was more active in the adsorption of N<sub>2</sub> than the raw material. They suggested that the formation of micropores and mesopores on the hydrochar surface during the carbonisation process was responsible for such an enhancement. In this line, the BET surface area of hydrochar is a critical feature to consider for

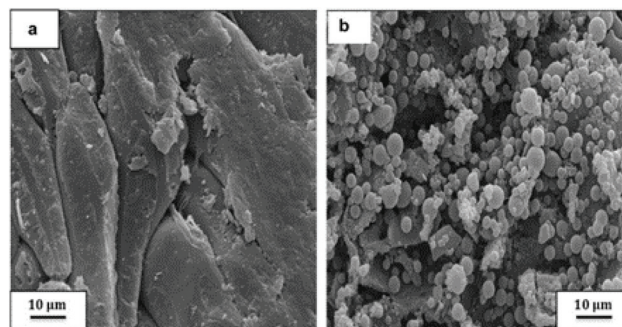


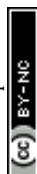
Fig. 4 SEM images showing the changes from the feedstock (a) to hydrochar (b). Adapted from Elaigwu *et al.*<sup>75</sup>

the commercial applications of this biomaterial. In this line, Nizamuddin *et al.*<sup>64</sup> found that tarry substances could hamper the production of hydrochar with a high BET surface area during the MA-HTC process.<sup>4,64,66,75</sup> However, the comparison between the BET areas of hydrochar produced by conventional HTC and MA-HTC developed by Li *et al.*,<sup>76</sup> revealed that when similar temperatures (180–240 °C) were used, the MA-HTC process yielded hydrochar with superior BET surface areas using much shorter reaction times. This finding highlights the inherent benefits of microwave irradiation.

## 4. Microwave-assisted hydrothermal liquefaction (MA-HTL) for bio-crude (bio-oil) production

The hydrothermal liquefaction (HTL) of biomass is a hydrothermal route, conducted at moderate temperatures (200–450 °C) and relatively high pressures (5–25 MPa), intended to convert biomass into a liquid product called bio-crude or bio-oil.<sup>99,100</sup> This process, conducted using water as the reaction medium, involves several reactions such as dehydrogenation, dehydration, decarboxylation, and deoxygenation. As a result, the biomass decomposes into reactive fragments, which further condense and repolymerise to produce a high energy-dense, crude-like oil, namely, bio-crude.<sup>16,101</sup> These transformations also lead to the formation of solid (hydrochar), aqueous, and gaseous products, similar to that described for the HTC of biomass.<sup>53</sup> But, the HTL process requires more severe processing conditions than the HTC of biomass.

The bio-crude produced by MA-HTL of biomass can be used in various fields, including energy generation and/or liquid biofuel and chemical (binder, adhesive, resin, and flavouring) production.<sup>102</sup> Besides, compared to other thermochemical processes for bio-crude/bio-oil production, such as fast pyrolysis, HTL has several inherent benefits. In particular, not only the HTL of biomass yields a liquid product with less oxygen and a superior HHV,<sup>103,104</sup> but also it is conducted at much lower temperatures. Besides, the utilisation of water as a



reaction medium dispenses with the need to dry the feedstock. These factors not only substantially contribute towards the energy efficiency of the process, but also make MA-HTL a very sustainable technique for biomass valorisation.<sup>4,103</sup> However, the bio-crude produced might be unsuitable as a 'drop-in' fuel due to low heating value, instability and high viscosity, properties inherited from the presence of oxygen-containing compounds.<sup>105</sup> A very appealing option to use this fraction as a fuel is oxygen reduction *via* hydrodeoxygenation (HDO).<sup>106–109</sup>

Given these promising features, a lot of work has been conducted on biomass HTL since it was firstly developed in the 1930s.<sup>110</sup> As an effort to improve the energy efficiency of the process and to take advantage of the excellent capability of water to absorb microwave radiation, in 2006 Kržan *et al.*<sup>111,112</sup> reported the microwave-assisted hydrothermal liquefaction (MA-HTC, also called direct liquefaction) of biomass using microwave irradiation to achieve hydrothermal conditions for the first time. Since then, quite a substantial work has been conducted on this matter due to the inherent benefits of running a hydrothermal process using microwave heating. These include the time- and energy-saving features of this method, the excellent controllability of the process, along with the extreme purity and high yields of the desired products compared to conventional heating.<sup>53,113–115</sup> In the scope of this section, the following will focus on the effects of the MA-HTL processing conditions and the type of biomass on the yields and properties of the bio-crude produced. The former include the impacts of the temperature, time, pressure, solid/water ratio, catalyst (type and amount) and microwave power. At the same time, the latter comprises the effects on the process of using different feedstocks such as pine and

spruce,<sup>103</sup> bamboo,<sup>116</sup> chicken cork waste,<sup>117</sup> brewers' spent grains (BSG),<sup>118</sup> straws, microalga (marine red seaweed), spent coffee grounds and sawdust.<sup>119</sup> All these studies reported to date suggest that MA-HTL is not only a potential alternative technology with a great development prospect for the manufacturing of biofuels and/or bio-chemicals from second and third biomass generations, but also an excellent niche for further research.<sup>53</sup>

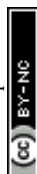
#### 4.1 Effect of the operating conditions on the yield and physicochemical properties of bio-crude

The HTL of biomass is a complex route involving various reactions. In general, the process can be divided into three stages: (i) the depolymerisation of the feedstock by hydrolysis; (ii) the formation of highly reactive species/fragments from decomposed biomass *via* dehydration, decarboxylation, and deamination, which then evolve towards the formation of bio-crude (bio-oil) and/or gas, and, (iii) the repolymerisation and/or recondensation of the reactive fragments to yield complex solid species (hydrochar and/or coke).<sup>118,120</sup> The yield and physicochemical properties of the bio-crude produced by MA-HTL are influenced by the conditions (temperature, time, catalyst, solid/water ratio and microwave power) and the type of biomass. These influences are summarised in Table 5 and discussed as follows.

**4.1.1 Reaction temperature.** Temperature plays a crucial role in the conversion of biomass to bio-crude during the MA-HTL process. By now, it is generally accepted that a moderate temperature contributes to the degradation of the feedstock into bio-crude. Alternatively, the use of a high temperature promotes the repolymerisation or depolymerisation of

**Table 5** Summary of the literature pertaining to microwave-assisted hydrothermal liquefaction of biomass

Biomass	Reaction parameters	Catalyst	Major results	Reference
Pine and spruce	Temperature (150–250 °C), pressure (50–120 bar), time (0–2 h), biomass loading (1 : 50).	Ni-Co/Al-Mg	Total biomass conversion and the gas and bio-crude yields are 13–77%, 7–67% and 1–29%, respectively	Remón <i>et al.</i> <sup>103</sup>
Softwood	Temperature (160–210 °C), time (5–20 min), power (300 W), biomass loading (1 : 75 (g mL <sup>-1</sup> ))	H <sub>2</sub> SO <sub>4</sub>	The highest lignin yield was obtained at 10 min and 190 °C	Zhou <i>et al.</i> <sup>122</sup>
Microalgae, marine red seaweed, spent coffee ground and sawdust	Temperature (270 °C), time (20 min), biomass loading (1 : 9)	NaCl	Biocrude yields were ~30 wt% (microalgae), ~17 wt% (marine red seaweed), ~25 wt% (spent coffee) and 7.9–27.1% (ground and sawdust)	Yang <i>et al.</i> <sup>119</sup>
Chicken carcasses	Temperature (120–240 °C), time (2 h), power (400 W), biomass loading (20/45 g mL <sup>-1</sup> )	—	The highest yield (59.41%) of bio-crude was obtained at 240 °C	Zhang <i>et al.</i> <sup>117</sup>
Microcrystalline cellulose and xylose (1 : 1) soy protein, soybean oil, alkaline lignin	Temperature (270 °C), time (20 min), biomass loading (1 : 11)	—	The yields of bio-crude were 16.3 ± 0.9 (protein), 10.2 ± 1.6 (saccharide), 2.7 ± 0.8 (lignin), and 103.8 ± 0.2 (lipids), respectively	Yang <i>et al.</i> <sup>123</sup>
Bamboo	Temperature (120–180 °C), time (3 min), power (550 W), biomass loading (1 : 4)	H <sub>2</sub> SO <sub>4</sub>	The highest conversion was 56.41% at 180 °C in water	Xie <i>et al.</i> <sup>116</sup>
Brewers' spent grains (BSG)	Temperature (180–250 °C), time (0–2 h), biomass loading (1 : 20)	Ni-Co/Al-Mg	The overall conversion and the yields of gas, aqueous fraction and bio-oil were 31–68%, 10–33%, 9–48% and 4–14% with various conditions, respectively	Lorente <i>et al.</i> <sup>118</sup>
Bagasse	Temperature (105 °C), time (4 h), biomass loading (1 : 15)	H <sub>2</sub> SO <sub>4</sub> , CH <sub>3</sub> COOH	The highest lignin yield (78.69%) is obtained after 30 min	Li <i>et al.</i> <sup>113</sup>



reactive biomass fragments, which forms solid or gas species, respectively, and reduces the bio-crude yield.<sup>104,118</sup>

The effect of the temperature on the bio-crude yield during the MA-HTL of biomass has been analysed by several authors. Liu *et al.*<sup>115</sup> studied the yield of aqueous products produced by the MA-HTL of rice straw. They found that the total organic carbon displayed an initial increasing tendency (from 2.01 to 5.71 g L<sup>-1</sup>), increasing the temperature from 150 to 190 °C. Still, the liquid carbon yield decreased to 5.4 g L<sup>-1</sup> with a subsequent temperature increment up to 230 °C. In another study, Lorente *et al.*<sup>118</sup> studied the influence of several operating conditions (temperature, time, solid/water ratio and catalyst loading) on the MA-HTL of brewers spent grains (BSG) using a Ni-Co/Al-Mg catalyst. They reported that the effect of the temperature on the bio-crude yield depended on the reaction time and the amount of catalyst. For a short reaction time (0 h) and in the absence of a catalyst, an increase in the reaction temperature (180–220 °C) increased the gas and aqueous fraction and bio-crude (bio-oil) yields. In contrast, a further increase (up to 250 °C) dropped the bio-crude yield, and a trend-off took place for the gas and liquid yields. These developments revealed that the bio-crude produced from biomass could be subsequently transformed into solid species (hydrochar) when high temperatures are used. Different trends for these yields were observed when the MA-HTL was conducted using a 2 h reaction time. In this case, a first increase in the temperature from 180 to 220 °C slightly increased the yields of the gas, bio-crude and aqueous phase. Additionally, a subsequent temperature increment up to 250 °C substantially increased the gas yield and produced a slight drop in the bio-crude yield without significantly influencing the aqueous fraction yield. These results suggested that part of the bio-crude could be transformed into gas when MA-HTL is conducted at high temperature and using long reaction times. These developments are in line with the work of Xie *et al.*,<sup>116</sup> who found that increasing the temperature up to 180 °C led to a linear increment in the yield of bio-crude. Nevertheless, other different trends have been reported in the literature. For example, Zhang *et al.*<sup>117</sup> addressed the MA-HTC of chicken crack wastes and indicated that the bio-crude yield increased differently depending on the temperature. Firstly, it augmented rapidly on increasing the temperature up to 160 °C, and then slowly until a maximum (59.41%) was reached at 240 °C. These differences may be a result of the non-lignocellulose character of this feedstock. In another study, Remón *et al.*<sup>103</sup> addressed the MA-HTL of a mixture of pine and spruce using a Ni-Co/Al-Mg catalyst. They found that the effect of the temperature depended on the reaction time. When a short reaction time (0 h) was used, the bio-crude yield was meagre and unaffected by the reaction temperature. Conversely, for a 2 h MA-HTL, increasing the temperature resulted in a substantial increase in the bio-crude yield, with distinctive developments taking place with and without a catalyst. These authors indicated that some of these trends were also observed in conventional liquefaction.<sup>118</sup> Thus, according to the above literature, the MA-HTL of biomass is such a complicated process, and

the optimum temperature should be determined based on the feedstock, catalyst, and other operating conditions.

**4.1.2 Reaction time.** Reaction time is another crucial factor affecting the bio-crude yield, whose impact can also depend on the temperature. In general, the yield of bio-crude increases with increasing reaction time. Nevertheless, this trend depends on the temperature, as high temperatures also promote bio-crude conversion into gases and/or solid species, thus diminishing the bio-crude yield.

Many authors have covered the impact of these influences on the process. According to Li *et al.*,<sup>113</sup> the bio-crude yield initially increased within the first minutes of the reaction, then reached a peak (78.69%) and finally slightly decreased due to the condensation of small molecules. Similar results were obtained by Feng *et al.*,<sup>114</sup> who proved that the yield of liquified products reached a maximum (86 wt%) within the initial 40 min of the process and then decreased down to 20.17% when reaction times longer than 50 min were used. Liu *et al.*<sup>115</sup> found that the TOC (total organic carbon) of the aqueous phase increased from 3.71 to 4.28 g L<sup>-1</sup> with increasing residence time from 5 to 10 min, but then it decreased to 3.89 g L<sup>-1</sup> when the MA-HTL process was conducted for more than 30 min.

In addition to the individual influence of the reaction time, it is important to bear in mind the existence of significant interactions between this variable and temperature. For example, Remón *et al.*<sup>103</sup> found that the reaction time did not substantially influence the gas or bio-crude yields at a low temperature (150 °C). In contrast, when the process was conducted at a high temperature (250 °C), the bio-crude yield increased with prolonging the reaction time between 0 and 1 h and then stabilised when longer reaction times (up to 2 h) were used. In another study, Lorente *et al.*<sup>118</sup> reported that increasing the reaction time from 0 to 2 h significantly reduced the bio-crude yield regardless of the temperature. They found that the interaction between the reaction time and temperature was not significant for the bio-crude yield; however, it was for the gas and aqueous phase yields. Different outcomes were observed depending on the combination of temperatures and times used in the MA-HTL process.

**4.1.3 Catalyst.** The main objectives of a catalyst are to reduce the formation of solid species (hydrochar) and to increase the liquid yield and quality. Furthermore, the addition of a catalyst can also help decrease the reaction temperature and pressure and reduce the reaction time.<sup>4</sup> The catalysts commonly used for the HTL of biomass comprise homogeneous alkali salts (Na<sub>2</sub>CO<sub>3</sub>, BaOH<sub>2</sub>, CaOH<sub>2</sub>, K<sub>2</sub>CO<sub>3</sub>, and KHCO<sub>3</sub>) and acids (H<sub>2</sub>SO<sub>4</sub>, HCOOH, CH<sub>3</sub>COOH) along with heterogeneous metals (Pt, Ni, Ru, and Pd) supported on metal oxides (MnO, MgO, NiO, ZnO, CeO<sub>2</sub>, and La<sub>2</sub>O<sub>3</sub>), zeolites or carbon nanotubes.<sup>103,104</sup>

However, work covering the use of a catalyst for the MA-HTL of biomass is scarce as this technology is still in an early development stage. In general, it has been reported that increasing the catalyst loading promoted the hydrolysis of biomass, which consequently helped increase the bio-crude



yield. In this regard, Li *et al.*<sup>113</sup> extracted lignin from bagasse using oxalic acid as a catalyst, and found that an increase in the amount of catalyst promoted the liquefaction yield, which was at its highest when a catalyst concentration of 15 vol% was used. Interestingly, an increase in the catalyst loading did not significantly influence the liquefaction yield. In another work, Remón *et al.*<sup>103</sup> produced bio-crude from a mixture of pine and spruce biomass and found that the addition of a catalyst (Ni-Co/Al-Mg) had no significant influence on the overall biomass conversion. However, the catalyst greatly affected the overall distribution of reaction products (yield of gas and bio-oil/bio-crude) and the bio-crude properties. Similar results were also reported by Lorente *et al.*<sup>118</sup> when used the same catalyst for the MA-HTL of BSG. These developments were accounted for by the heterogeneous nature of the catalyst, which resulted in mass transfer limitations between the catalyst and the solid biomass. Still, the presence of a catalyst promoted the hydrolysis and gasification of depolymerised liquid species formed during the treatment.<sup>46</sup>

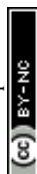
The literature reported to date shows that, in general, the bio-crude yield is more affected by the processing conditions in comparison to the hydrochar yield. These differences might be accounted for by the number and type of chemical transformations involved in the production of bio-crude or hydrochar. During the MA-HTL of biomass, the bio-crude can be produced from different fractions and also evolve towards various products. For example, part of the bio-crude can be converted into gas and/or repolymerise to produce solid species. Besides, the bio-crude and the aqueous phase are in equilibrium, and some organics can shift from the liquid phase to the bio-crude and *vice versa*. However, more work addressing the effects of the processing variables and interactions between variables is needed to gain more insights into the impact of the conditions on the yields of bio-crude and hydrochar.

**4.1.4 Other factors: solid/water ratio, biomass type, pressure and microwave power.** The solid (biomass)/water (solvent) ratio significantly influences the amount of bio-crude produced during the MA-HTL of biomass. In the vast majority of the studies conducted, bio-crude production is favoured using low solid/water ratios. However, the energetic aspects of the process must also be evaluated, and the right balance should be struck. A low biomass loading requires more energy to be used for heating water, which also increases the costs of possible wastewater treatments.<sup>104</sup> The effect of this variable on the bio-crude yield has been assessed by several authors. Guo *et al.*<sup>121</sup> reported that the liquefaction yields initially increased sharply with decreasing solid/water ratio (*i.e.*, increasing the water/solid ratio). Then a trend-off was observed with a further increase in the water/solid ratio.

Pressure, particle size and microwave power are also important parameters that influence the efficiency of the process, thus controlling both the distribution of the overall reaction products (gas, bio-crude, hydrochar and aqueous fraction) and the properties of each fraction. In the vast majority of the studies addressing the MA-HTL of biomass, the effect of the

pressure was not analysed independently as they were carried out under autogenous pressure. However, Remón *et al.*<sup>103</sup> and Lorente *et al.*<sup>118</sup> examined the effect of the pressure independently. They reported that increasing the MA-HTL treatment pressure reduced the dielectric loss factor of water, which limited the microwave efficiency. This promoted the formation of chemicals produced at early reaction stages (*e.g.* water-soluble sugars) and decreased the yields of bio-crude and gas at the expense of the formation of water-soluble species. The effect of the particle size also influences the efficiency of the MA-HTL process. In particular, the microwave efficiency increases with biomass small particle sizes, which also helps decrease the amount of solvent required to achieve the same conversion degree. This is in good agreement with the work of several authors, who have reported that the bio-crude yield increased as the solid particle size of the processed biomass decreased.<sup>112,124</sup> Also, the microwave power also determines the distribution of the overall reaction products. Guo *et al.*<sup>121</sup> revealed that augmenting the microwave power from 200 to 400 W led to a gradual increase in the liquefaction (bio-crude) yield. At the same time, a subsequent increase from 400 to 600 W diminished the bio-crude production at the expense of the formation of hydrochar, as the use of high microwave power promoted the carbonisation of the bio-crude produced.

The yield and physicochemical properties of the bio-crude produced during the MA-HTL depend on the type of biomass, due to the intrinsic differences in structural compositions between biomasses in terms of saccharides (cellulose and hemicellulose), lignin, proteins, and lipid contents. This not only does influence the overall reaction pathway of the process individually, but also modifies the individual decomposition behaviour of each structural compound as possible interactions between them might affect the yields and properties of the reaction products.<sup>123</sup> Regarding the reactivity of each structural component alone, it has been found that higher bio-crude yields were produced with biomasses with high saccharide (cellulose and hemicellulose) contents, due to their easier degradation during the process in comparison to lignin. In contrast, a lower bio-crude yield was attained using biomasses with high proportions of this latter component due to its tendency to repolymerise.<sup>17</sup> With this in mind, Yang *et al.*<sup>119</sup> addressed the influence of the type of biomass on the bio-crude yield. In particular, they subjected four types of feedstocks with different compositions (*Chlorella* sp. red seaweed, spent coffee grounds, and sawdust) to MA-HTL, using water and seawater as the reaction media. They found that the yield and quality of the bio-crude substantially depended on the feedstock. In parallel work, Yang *et al.*<sup>123</sup> also processed four individual structural components (saccharide, lipid, protein, and lignin) along with their mixtures. They obtained various bio-crude yields and chemical compositions and detected several synergistic and antagonistic interactions. As such, these findings provided more pieces of evidence for the fact that the feedstock composition exerts a substantial influence on the MA-HTL process.



## 4.2 Characterisation of the bio-crude

**4.2.1 Elemental composition and higher heating value (HHV).** Table 6 compares the HHV of hydrochar and bio-crude produced by MA-hydrothermal carbonisation/liquefaction of biomass. It has been widely accepted that increasing the temperature, enlarging the reaction time and/or increasing the catalyst loading promote the development of deoxygenation and decarboxylation reactions. As a result of these transformations, the amounts of C, N, and H in the bio-crude increase and the proportion of O decreases, leading to a rise in the higher heating value (HHV) of the bio-crude. Lorente *et al.*<sup>118</sup> reported that increasing the temperature, enlarging the reaction time, and/or augmenting the catalyst loading during the MA-HTL of BSG increased the relative contents of C, N and H in the bio-crude and decreased the proportion of O because deoxygenation reactions took place to a more significant extent. Additionally, Remón *et al.*<sup>103</sup> revealed that among these factors, the catalyst loading was the most substantial variable affecting the composition and HHV of the bio-crude during the MA-HTL of a mixture of pine and spruce. In this case, the effect of the other processing conditions was only significant with high catalyst loadings. In addition, for biomasses with high protein content, the extension of the Maillard reaction was considered a key factor affecting the composition of bio-crude. Zhang *et al.*<sup>117</sup> reported that with high temperatures, the nitrogen content of the biomass was transferred to the bio-crude *via* the Maillard (amino compounds with sugars) and condensation (ammonia and fatty acids) reactions. These transformations resulted in the formation of N-heterocyclic compounds and amides in the bio-crude, which increased the proportion of N in this liquid.

**4.2.2 Chemical composition.** Biocrude produced during the HTL of biomass consists of a complex mixture of several compounds of different nature, including aldehydes, ketones, phenols, alkanes, fatty/carboxylic acids, and nitrogen compounds.<sup>125</sup> The presence and abundance of these species in bio-crude are directly linked to the composition of the raw material and the reaction conditions (temperature, time, pressure and catalyst type and loading) used in the HTL process. The chemical determination of these species in the bio-crude is complex, as this liquid also contains some high molecular weight compounds, primarily derived from lignin, that cannot be determined by Gas Chromatography (GC). Remón *et al.*<sup>103</sup> reported that only around 25 wt% of the compounds present in bio-crude obtained from lignocellulose biomass could be analysed by GC.

The MA-HTL of biomass includes a variety of complex reactions, involving hydrolysis, dehydration decarboxylation, deamination and polymerisation. Fig. 5 shows a possible reaction pathway showing some of the essential chemical transformations occurring during the MA-HTL of biomass. Cellulose and hemicellulose in biomass firstly depolymerise to oligomers *via* hydrolysis reactions. Then these oligomers are further hydrolysed into monosaccharides and subsequently converted to aldehydes under more severe conditions. Afterwards, these aldehydes can be converted to carboxylic acids, while insoluble humins can also be obtained *via* repolymerisation reactions.<sup>126</sup> The lignin fraction is transformed into phenolic compounds, through the cleavage of ether-bonds and hydrolysis reactions, and/or solid species *via* repolymerisation. Lipids are firstly hydrolysed into fatty acids, triesters and glycerol (triacylglycerides, TAGs) and then converted to alkanes and/or aldehydes/alcohols under alkaline conditions. The transformation of proteins starts with an initial hydrolysis reaction yielding amino acid units, which are then transformed to either carbonic acids and amines *via* decarboxylation or ammonia and carboxylic acids by deamination. At the same time, the amino acids can also react with monosaccharides through the Maillard reaction, leading to the formation of more nitrogen-containing chemical compounds.<sup>46,127–129</sup>

Given this complex reaction pathway, the chemical composition of bio-crude depends on the operating conditions used in the MA-HTL process and the nature of the feedstock. In general, a complete reaction (achieved by increasing the temperature, reaction time and catalyst loading) enhances the formation of phenols, thus decreasing the number of aldehydes and carboxylic acids, as the latter species are produced at early reaction stages.<sup>103</sup> More specifically, Zhang *et al.*<sup>117</sup> reported that an increase in the temperature reduced the total fatty acid content in the bio-crude. Additionally, Lorente *et al.*<sup>118</sup> also discovered that increases in the temperature, time and/or catalyst amount promoted biomass depolymerisation reactions. These transformations led to an increment in the proportion of low molecular weight species (furans, phenols, aldehydes, ketones and carboxylic acids) in the bio-crude at the expense of species produced at early reaction stages, such as aldehydes and carboxylic acids. In another study, Remón *et al.*<sup>103</sup> revealed

**Table 6** Comparison of HHVs of hydrochar and bio-crude

Products	Biomass	HHV (MJ kg <sup>-1</sup> )	Reference
Hydrochar	Rice straw	17.8	Nizamuddin <i>et al.</i> <sup>64</sup>
	Pig faeces	21.5–23.4	Wang <i>et al.</i> <sup>65</sup>
	Corn stock	22.82	Kang <i>et al.</i> <sup>66</sup>
	Rapeseed husk	21.57	Elaigwu <i>et al.</i> <sup>78</sup>
	Red seaweed	18.8–24.7	Cao <i>et al.</i> <sup>80</sup>
	Red macroalgae	14.93–18.07	Teh <i>et al.</i> <sup>82</sup>
	Green waste	17.91–23.01	Shao <i>et al.</i> <sup>67</sup>
	Palm kernel shell	27.63	Zainal <i>et al.</i> <sup>96</sup>
	Sugarcane bagasse	18.45–20.58	Chen <i>et al.</i> <sup>81</sup>
	Bamboo sawdust	18.27–20.83	Dai <i>et al.</i> <sup>70</sup>
	<i>Prosopis africana</i> shell	21.84–22.37	Elaigwu <i>et al.</i> <sup>84</sup>
Bio-crude	Brewers' spent grains	9–27	Lorente <i>et al.</i> <sup>118</sup>
	Microalgae, marine red seaweed, spent coffee ground and sawdust	24.3–32.0	Yang <i>et al.</i> <sup>119</sup>
	chicken carcasses	26.46	Zhang <i>et al.</i> <sup>117</sup>
	Pine and spruce	4–28	Remón <i>et al.</i> <sup>103</sup>



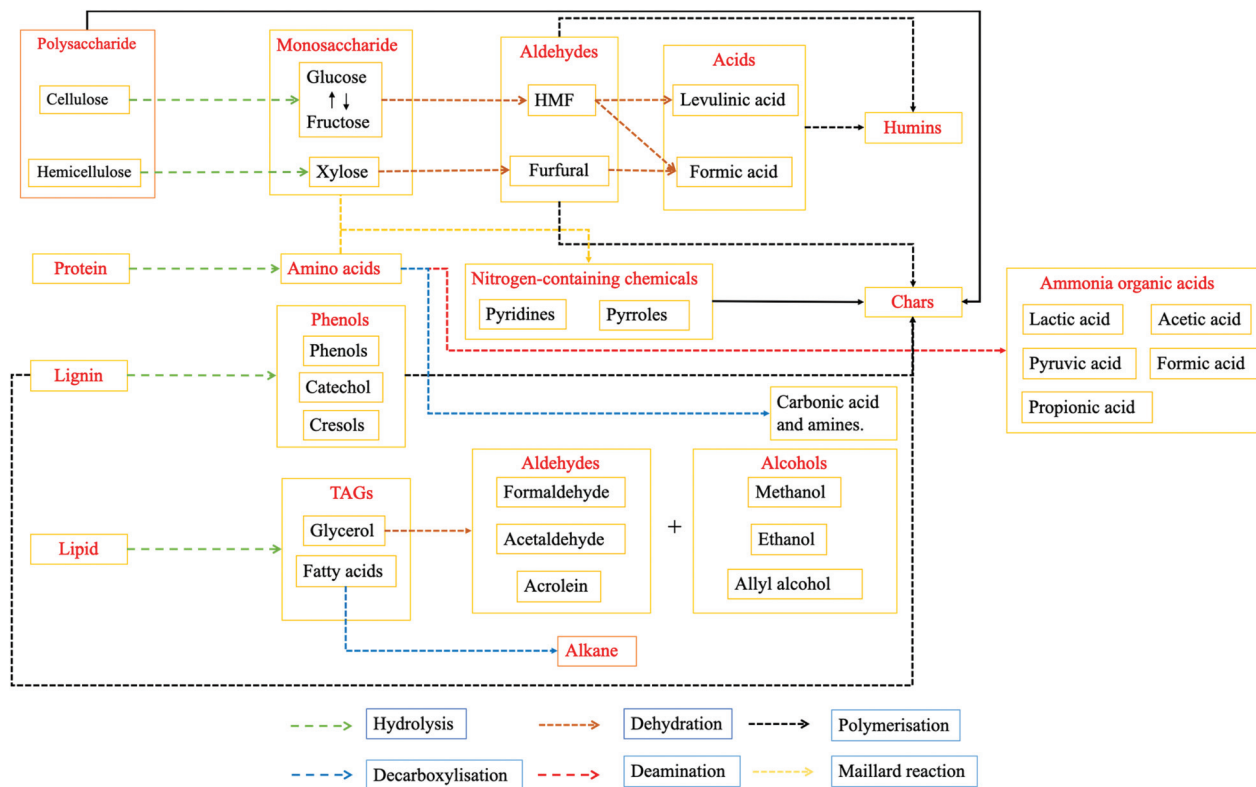


Fig. 5 Possible reaction pathway during the hydrothermal processing of biomass.

that more substantial extensions of isomerisation, cyclisation, and dehydration reactions increased the presence of phenols. They also dropped the relative number of species produced at early reaction stages, such as aldehydes and carboxylic acids. These results are also consistent with the FT-IR bio-crude characterisation data discussed in the next section. Yang *et al.*<sup>123</sup> investigated the bio-crude formation from four model compounds by MA-HTL, addressing how and to what extent each combination influenced the chemical composition of the bio-crude. The experimental results revealed that bio-crude with different compositions was obtained, thus confirming the significant effect of the feedstock on the process.

**4.2.3 Fourier transform infrared (FTIR) spectroscopy.** Bio-crude (bio-oil) is a remarkably complex mixture. Thus, considering the limitation described above for its determination using

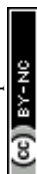
GC only, several authors have complemented this analysis with FTIR characterisation. The most common bands observed during the characterisation of bio-crude produced by MA-HTL are listed in Table 7. This information provides an excellent reference tool for the characterisation of these complex liquids.

## 5. Microwave-assisted hydrothermal treatment (MA-HTT) for the production of renewable value-added chemicals and biomaterials

Microwave-assisted hydrothermal treatment (MA-HTT) can also be used for the production of value-added chemicals and

Table 7 Common characteristic bands found in bio-crude identified by FTIR

Absorption band (cm <sup>-1</sup> )	Assignment	Component	Reference
3100–3500	O–H stretching vibration	Water, phenols, fatty acids	Zhuang <i>et al.</i> <sup>101</sup>
2925 and 2857	C–H stretching vibrations	Alkanes or fatty acids	Zhuang <i>et al.</i> <sup>101</sup>
1650–1730	C=O stretching	Ketones, aldehydes, carboxylic acids	Guo <i>et al.</i> <sup>101,121</sup>
1550–1490	NO <sub>2</sub> stretching	Nitrogenous compounds	Zhuang <i>et al.</i> <sup>101</sup>
1575–1525	N–H bending vibration	Amines and amides	Zhang <i>et al.</i> <sup>117</sup>
1470–1350	C–H bending	Aliphatic and alkyl aromatic compounds	Zhang <i>et al.</i> <sup>117</sup>
1300–950	C–O stretching alcohol	C–O stretching alcohol	Zhuang <i>et al.</i> <sup>101</sup>
1050–1200	O–H bending	Phenol, esters, ethers	Guo <i>et al.</i> <sup>121</sup>
915–650	O–H bending	Phenol, esters, ethers	Zhuang <i>et al.</i> <sup>101</sup>
880–680	C–H bending	Aromatic compounds	Guo <i>et al.</i> <sup>121</sup>



biomaterials.<sup>130</sup> As described above, the use of microwave heating to achieve hydrothermal conditions has several advantages over conventional heating, primarily including time and energy savings and higher product yields.<sup>80,128</sup> During the MA-HTT, biomass decomposes into valuable water-soluble compounds, which can be used in a plethora of applications. This section lists the work reported to date on the use of MA-HTT for the manufacture of valuable products and biomaterials, carefully addressing the effects of the processing conditions and biomass type. Table 8 summarises the literature addressing the MA-HTT of biomass for the production of value-added liquid compounds.

Bio-alcohol production from lignocellulosic biomass-derived sugars has attracted widespread interest owing to the inherent benefits of this method, *i.e.*, it is renewable, economical, and environmentally friendly.<sup>131</sup> Biological fermentation of sugars is a possible way to produce bioenergy; however, the intrinsic recalcitrant structure of biomass (coexistence of lignin in the plant cell and the high crystallinity degree of cellulose) hinders the direct fermentation of biomass. Thus, a pretreatment step is necessary to prepare biomass for a subsequent fermentation process.<sup>132</sup> This preparation step comprises the removal of lignin and the decrease of cellulose crystallinity, along with an increase in the surface area and pore volume of the biomass. To this end, several pretreatment technologies have been used over the past few years, such as physical (*e.g.* grinding, ball milling, extrusion, chip, and pressing), chemical (*e.g.* acids, ionic liquids, alkali, organic solvents, metal chlorides), physicochemical (*e.g.* steam explosion, supercritical CO<sub>2</sub>, plasma) and biological (*e.g.* fungal, microbial, and enzyme) treatments. Each method has its own merits and demerits. For instance, physical treatment is highly energy-consuming and not very good at lignin removal; chemical methodologies (acids and alkalis) could not be environmentally friendly depending on the acid/base used, while biological processes are very lengthy and not very efficient in terms of the yield of desired products.<sup>162</sup>

Given these drawbacks, Ooshima *et al.*<sup>163</sup> proposed, for the first time, the use of the MA-HTT of biomass as a pretreatment step for biomass fractionation of hardwoods and softwoods. Since then, a lot of work has been conducted as this technology is considered superior in terms of effectiveness and product selectivity to other technologies. Besides, it is more controllable, energy-efficient and time-saving.<sup>45</sup> This excellent process controllability allows maximising the sugar yield as well as minimising the number of inhibiting fermenting compounds (*e.g.* furfural, HMF, acetic and formic acids, and phenolic compounds). This strategy has been used to produce saccharide-rich aqueous solutions for subsequent fermentation processes. The work reported to date on the effect of processing conditions on biomass conversion into fermentable saccharides is described as follows.

## 5.1 Effect of the operating conditions on the yield of sugars

**5.1.1 Reaction temperature.** Temperature exerts a dual effect on the process and must be controlled carefully. On the

one hand, high temperatures promote the hydrolysis of polysaccharides into fermentable saccharides. On the other hand, they also favour the subsequent decomposition of the latter species into secondary products, such as furfural, HMF and carboxylic acids, and boost lignin depolymerisation yielding phenolic compounds. All these species are common inhibitors for most of the yeasts used for saccharide fermentation.<sup>164,165</sup> Therefore, as temperature plays a crucial role in the saccharide yield and purity, the effect of this variable has been carefully studied and reported in the literature. López-Linares *et al.*<sup>133</sup> studied the MA-HTT of brewer's spent grains (BSG) for sugar production. The experimental results indicated that the optimum temperature and time were 192.7 °C and 5.4 min, respectively: conditions under which it was possible to recover in the enzymatic hydrolysate up to 64 wt% of the total hemicellulosic sugars and 70% of all the recoverable glucose. Similarly, Mihiretu *et al.*<sup>146</sup> processed aspen wood and found that the maximum xylan yield (*ca.* 66.1%) was obtained at 195 °C by conducting MA-HTT for 20 min. Xu *et al.*<sup>166</sup> explored the MA-HTT of eucalyptus biomass using acidic ionic liquids as catalysts. They found that increasing the temperature positively influenced the yield of the xylose monomer between 150 and 190 °C, as it increased from 2.52 to 49.58 mg g<sup>-1</sup>, and exerted a negative impact above 200 °C due to the progressive degradation of xylose at high temperature. Yuan *et al.*<sup>148</sup> reported that the yield of hemicellulose presented an initial gradual increase (41.26 to 68.40 mg g<sup>-1</sup>) as the temperature increased from 160 to 180 °C, and then upsurged sharply to 105.15 mg g<sup>-1</sup> when the temperature reached 200 °C. They explained that this pronounced increase was due to the lower pH and more effective diffusion capability of water at a higher temperature. Luo *et al.*<sup>167</sup> also found that the highest hemicellulose conversion took place at 200 °C. Sasaki *et al.*<sup>142</sup> obtained the highest glucose yield (0.48 g/g) during the MA-HTT of *Styrax tonkinensis* wood at 200 °C for 1 min using 1% (w/w) of sulfuric acid as a catalyst. Yuan *et al.*<sup>141</sup> conducted an acid MA-HTT of *Ascophyllum nodosum*, found an optimum temperature at 150 °C, and reported a progressive reduction in the monosaccharide yield at 180 °C.

**5.1.2 Reaction time.** Reaction time also exerts a significant influence on the sugar yield. Besides, its relative impact relies on the processing temperature. At low temperature, the effect of the reaction time is relatively weak. In contrast, the combination of high temperatures and long reaction times (high process severity) results in a synergistic increment in the reaction rate of hydrolysis and secondary reactions. The latter diminishes the yield of sugars and increases the presence of side products. Therefore, these data suggest that the best processing variable combination is the use of a relatively high temperature for a short reaction time to maximise the saccharide content and diminish the subsequent transformation of these species into degradation/secondary products.<sup>146</sup>

Several authors have addressed the effect of the reaction time on the oligosaccharide production by MA-HTT of biomass. Deng *et al.*<sup>149</sup> extracted xylo-saccharides from corncob and reported that increasing the reaction time



**Table 8** Microwave-assisted hydrothermal treatment of biomass for value-added chemical production

Products	Biomass	Reaction parameters	Catalyst	Results	Reference
Sugars	<i>Ficus religiosa</i> leaves	Temperature (85–109 °C), time (2–15 min), biomass loading (1 : 20 m/m)	HCl	Higher (10.1 wt%) glucose yield was achieved compared to the conventional process (4.1 wt%)	Klein <i>et al.</i> <sup>131</sup>
	Brewer's spent grains	Temperature (135.5–220 °C), time (20–35 min), biomass loading (1 : 10 m/m)	—	64% hemicellulosic sugar recovery and 70% glucose recovery were obtained at 192.7 °C and 5.4 min	López-Linares <i>et al.</i> <sup>133</sup>
	Sorghum bagasse	Temperature (100–160 °C), time (60 min), biomass loading (1 : 8 m/m)	Ammonium hydroxide	The best glucose yield (42%) and ethanol yields (21%) were obtained at 130 °C for 1 h	Chen <i>et al.</i> <sup>134</sup>
	Areca nut husk	Time (1 and 3 min), power (180, 540, 900 W)	NaOH	The maximum hemicellulose yield (52%) was obtained at 900 W and 3 min	Singh <i>et al.</i> <sup>135</sup>
	Microalgae	Temperature (80–140 °C), time (12 min), biomass loading (1 : 10 m/m)	—	Microwave technique increased the lipid recovery (from 0.5 to 1.4 wt%)	Biller <i>et al.</i> <sup>136</sup>
	Eucalyptus	Temperature (140–200 °C), biomass loading (1 : 10 m/m)	[bmim]HSO <sub>4</sub>	5.04 wt% of xylooligosaccharides and 26.72 wt% of xylan were achieved. 89.2% glucose conversion with a 64.9% solid recovery	Xu <i>et al.</i> <sup>137</sup>
	Sago pith waste	Time (1–5 min), power (550–900 W), biomass loading (1 : 12 m/m)	CO <sub>2</sub>	The highest theoretical yield of glucose (43.8%) and ethanol (40.5%) was obtained	Thangavelu <i>et al.</i> <sup>138</sup>
	Cotton waste	Temperature (180–200 °C), time (1–15 min), biomass loading (1 : 40 m/m)	H <sub>2</sub> SO <sub>4</sub>	The highest glucose yield was 28.9%, obtained at 200 °C for 7 min	Sasaki <i>et al.</i> <sup>139</sup>
	Sago pith waste	Time (1–3 min), power (550–900 W), biomass loading (1 : 15 m/m)	H <sub>2</sub> SO <sub>4</sub> and HCl	The highest glucose yield (88%) was obtained at 900 W for 1 min with 1.0 mol L <sup>-1</sup> H <sub>2</sub> SO <sub>4</sub>	Thangavelu <i>et al.</i> <sup>140</sup>
	<i>Ascophyllum nodosum</i>	Temperature (120–180 °C), time (0–30 min), biomass loading (0.6%–6%, w/v)	H <sub>2</sub> SO <sub>4</sub>	The highest yield of monosaccharides (127 mg g <sup>-1</sup> ) was obtained at 150 °C for 1 min with 0.4 M H <sub>2</sub> SO <sub>4</sub> and 3.13% (w/v) biomass concentration	Yuan <i>et al.</i> <sup>141</sup>
	Bode ( <i>Styrax tonkinensis</i> ) wood	Temperature (180–200 °C), time (1–5 min), biomass loading (1 : 20 m/m)	H <sub>2</sub> SO <sub>4</sub>	The highest yield (0.48 g/g) of glucose was obtained at 200 °C for 1 min with 1.0 wt% H <sub>2</sub> SO <sub>4</sub>	Sasaki <i>et al.</i> <sup>142</sup>
	Sugarcane bagasse	Temperature (170 ± 5 °C), time (3–10 min), biomass loading (1 : 40 m/m)	NaOH/H <sub>2</sub> SO <sub>4</sub>	The highest sugar yield (86%) was achieved using 0.2 M H <sub>2</sub> SO <sub>4</sub> for 7 min	Zhu <i>et al.</i> <sup>143</sup>
	Sago palm bark	Time (5–15 min), power (80–800 W), biomass loading (1 : 10–1 : 20 m/m)	H <sub>2</sub> SO <sub>4</sub> , NaOH, NaHCO <sub>3</sub>	Diluted acid/alkali concentrations, low temperature and short reaction times increased the digestibility of the lignocellulosic material for the following hydrolysis process	Ethaib <i>et al.</i> <sup>144</sup>
	Pineapple peel	Time (5–20 m), power (90–900 W), biomass loading (100–160 g L <sup>-1</sup> )	—	The highest total sugar yield (80.2%) was obtained at 900 W for 9 minutes using 100 g L <sup>-1</sup> biomass loading	Chongkhong <i>et al.</i> <sup>145</sup>
	Aspenwood sawdust and sugarcane trash	Temperature (170–200 °C for aspen wood and 165–195 °C for sugarcane trash), time (8–22 min), biomass loading (1 : 1 m/m)	—	The highest xylan extraction yields (66% and 50%) and cellulose digestibilities (78 and 74%) were obtained from aspen wood and sugarcane trash, respectively	Mihiretu <i>et al.</i> <sup>146</sup>
	Pubescens powder	Temperature (140–216 °C), biomass loading (1 : 20 m/m)	—	The highest dissolution of hemicellulose (more than 95%) was obtained at 200 °C	e Silva <i>et al.</i> <sup>147</sup>
	Tobacco biomass	Temperature (120–200 °C), time (0–40 min), biomass loading (1 : 20 m/m)	—	The best condition for hemicellulose extraction from extracted non-structural carbohydrates was 200 °C and 0 min, and the yield was 105.15 mg g <sup>-1</sup> .	Yuan <i>et al.</i> <sup>148</sup>
	Corn cob	Temperature (130–150 °C), time (0–40 min), biomass loading (1 : 20 m/m)	—	The maximum yield of xylo-sugars (86.10%) was obtained at 130 °C for 30 min	Deng <i>et al.</i> <sup>149</sup>
	Cassava pulp and tapioca flour	Temperature (180–240 °C), time (5–18 min), biomass loading (1 : 20 m/m)	Activated carbon	The highest glucose yield (52.27%) was obtained from cassava pulp at 210 °C for 15 min	Hermiati <i>et al.</i> <sup>150</sup>
	Sugarcane bagasse	Temperature (90 °C), time (20–40 min), biomass loading (1 : 25 m/m)	H <sub>2</sub> SO <sub>4</sub>	The highest yield of XOS was 290.2 mg g <sup>-1</sup> with 0.24 M H <sub>2</sub> SO <sub>4</sub> for 31 min	Bian <i>et al.</i> <sup>151</sup>
	Beech wood hemicellulose	Temperature (140–210 °C), time (0–60 min), biomass loading (1 : 4–1 : 20 m/m)	—	The result is 81% liquid yield and 96 C-wt% XOS purity, which was obtained at 172 °C, 1 : 20 m/m biomass loading for 47 min	Remón <i>et al.</i> <sup>152</sup>
	Rapeseed meal	Temperature (150–210 °C), time (0–60 min)	CH <sub>3</sub> COOH	The best condition for lignin solid (85 wt%) and a water solution with rich oligosaccharide obtained at 186 °C for 2 min	Remón <i>et al.</i> <sup>153</sup>



Table 8 (Contd.)

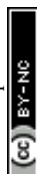
Products	Biomass	Reaction parameters	Catalyst	Results	Reference
HMF, furfural and carboxylic acids	Carnauba leaves, macauba pulp, macauba shell and pine nutshell	Temperature (120–200 °C), time (5–60 min)	TiO <sub>2</sub>	The highest production yield of HMF/furfural was 53.24%	da Silva Lacerda <i>et al.</i> <sup>154</sup>
	Wheat straw, triticale straw and flax shives	Temperature (140–190 °C), time 1–30 min, biomass loading (1 : 5–1 : 200 m/m), pH (2–0.13)	HCl, H <sub>2</sub> SO <sub>4</sub> , H <sub>3</sub> PO <sub>4</sub> , HNO <sub>3</sub> , CH <sub>3</sub> COOH, HCOOH	Furfural yields were 48.4% (wheat straw), 45.7% (triticale straw), and 72.1% (flax shives), respectively at 180 °C for 20 min with 0.1 M HCl and 1 : 100 m/m biomass loading	Yemiş <i>et al.</i> <sup>128</sup>
	Sugarcane bagasse	Temperature (130–190 °C), time (1–60 min), biomass loading (1 : 8–1 : 20 m/m)	HCl	The highest HMF yield (8.1 wt%) was obtained at 149 °C, 4 min and liquid/solid 12 : 1 m/m ratio	Shao <i>et al.</i> <sup>155</sup>
	Corn stover	Temperature (180–200 °C), time (10–30 min), biomass loading (1 : 20 m/m)	Niobium phosphate	Optimised furfural yields up to 23% at 170 °C for 30 min	Bernal <i>et al.</i> <sup>156</sup>
	Giant reed	Temperature (140–190 °C), time (5–45 min), biomass loading (7 : 100 m/m)	—	Giant reed represents a promising prospect of FA (70%) and LA (90%) theoretical yield	Antonetti <i>et al.</i> <sup>44</sup>
	Corn cob	Temperature (160–190 °C), time (0–50 min), biomass loading (1 : 20 m/m)	SnCl <sub>4</sub>	The highest furfural yield (9.0 wt%) was obtained at 190 °C with 1 wt% SnCl <sub>4</sub>	Ren <i>et al.</i> <sup>157</sup>
	Wheat straw	Temperature (140–200 °C), time (1–41 min), pH (0.1–2.1) biomass loading (15–195 mL g <sup>−1</sup> )	HCl	The highest yields of furfural, HMF, xylose and glucose were 66%, 3.4%, 100%, and 65%, respectively	Yemiş <i>et al.</i> <sup>158</sup>
	Corn stover, switchgrass, lodgepole pine and poplar	Temperature (180–210 °C), time (0–10 min), biomass loading (1 : 100 m/m)	Maleic acid	The highest yield (61%) of furfural was obtained at 200 °C for 28 min from corn stover	Kim <i>et al.</i> <sup>159</sup>
	Potato peel waste and fungus sporocarps	Temperature (140–180 °C), time (15–60 min), biomass loading (1 : 10 m/m)	H <sub>2</sub> SO <sub>4</sub> , CrCl <sub>3</sub> ·6H <sub>2</sub> O or AlCl <sub>3</sub> ·6H <sub>2</sub> O	The highest levulinic acid yield (49%) from potato peel waste was obtained at 180 °C, 15 min, with 0.5 M H <sub>2</sub> SO <sub>4</sub> and 0.0075 M CrCl <sub>3</sub> , respectively. 62% yield from <i>Cortinarius armillatus</i> was obtained at 180 °C, 40 min with 0.5 M H <sub>2</sub> SO <sub>4</sub> and 0.0075 M CrCl <sub>3</sub> , respectively	Lappalainen <i>et al.</i> <sup>160</sup>
	Seaweed-derived agarose	Temperature (180 °C), time (5–30 min), biomass loading (1 : 25 m/m)	H <sub>2</sub> SO <sub>4</sub> , MgCl <sub>2</sub>	The highest HMF (51%, without a catalyst) and LA (64%, with 1 wt% H <sub>2</sub> SO <sub>4</sub> ) yields were obtained at 180 °C for 10 min	Francavilla <i>et al.</i> <sup>161</sup>

(0–40 min) increased the xylose yield (from 20.63% to 74.72%) at 130 °C. A similar trend was also obtained at 140 °C, while at 150 °C, the xylose yield decreased when long reaction times were used (69.20 at 30 min and 56.36% at 40 min), due to the degradation of xylose into byproducts. Klein *et al.*<sup>131</sup> studied the MA-HTT of *Ficus religiosa* leaves for bioethanol production and observed that an initial increase in the reaction time (from 2 to 8 min) led to an increment in the glucose yield (from 4.8 to 9.1 wt%). Conversely, a further time increment (8–15 min) reduced the glucose yield (about 7%) due to the formation of insoluble humins from the condensation of the HMF yielded from the dehydration of glucose. Sasaki *et al.*<sup>139</sup> addressed the MA-HTT of cotton waste for glucose and valuable chemical production. These authors found that at 200 °C with 0.25 wt% sulfuric acid, the hydrolysed glucose yield increased (5.08–25.0 g) with prolonging the reaction time (1–7 min). A subsequent increase in the reaction time was detrimental, and the glucose yield decreased (20.8 g) after 7 min due to a progressive degradation into secondary products.

**5.1.3 Catalyst.** Minerals (H<sub>2</sub>SO<sub>4</sub> and HCl) and, to a lesser extent, carboxylic (CH<sub>3</sub>COOH) acids are the most used catalysts during the MA-HTT of biomass for oligosaccharide production.<sup>131,153</sup> These acids provide additional protons to

the reaction medium. This helps break down the strong chemical bonds of polysaccharides, yielding soluble mono- and/or oligosaccharides. However, the catalyst dosage must be carefully controlled as high acid concentrations may lead to the degradation of reducing sugars to undesirable byproducts, diminishing the yield of fermentable species and increasing the amounts of inhibitors in the hydrolysate.<sup>33,82</sup>

The effect of the type and acid concentration on the MA-HTT of biomass to produce fermentable species has been carefully discussed in the literature. Yuan *et al.*<sup>141</sup> found that the monosaccharide yield initially increased with increasing acid concentration (0.01–0.4 M H<sub>2</sub>SO<sub>4</sub>). However, the use of higher concentrations along with prolonged reaction times led to reductions in the sugar yield due to the formation of by-products. Similarly, Sun *et al.*<sup>168</sup> reported that the concentration of sulfuric acid displayed a positive effect on the glucose yield with low catalyst dosages. In contrast, the use of H<sub>2</sub>SO<sub>4</sub> concentrations greater than 0.04 M exerted a negative impact, as oligosaccharides were converted into secondary products. In another study, Remón *et al.*<sup>153</sup> used CH<sub>3</sub>COOH as a catalyst in the fractionation of rapeseed meal by MA-HTT. They found that an increase in the concentration of CH<sub>3</sub>COOH exerted a significant influence on the process. For the production of a



fermentable broth, they reported that an increase in the catalyst loading increased the amount of sugars in the liquid hydrolysate under some conditions and inhibited the formation of humins.

Besides, alkali salts and activated carbon have also been used as catalysts in this process. Tsubaki *et al.*<sup>45</sup> revealed that the halide salts of alkali and alkali earth metals improved the efficiency of the MA-HTL of biomass and reduced the energy consumption during the treatment by increasing the frequency factor of the reaction. Furthermore, in another study, these authors reported that NaCl effectively catalysed the MA-HTT of corn starch. The catalyst was capable of increasing the yield of reducing sugars by 1.14–1.15-fold using a much lower temperature (10–20 °C) than when the process was conducted in the absence of a catalyst.<sup>43</sup> Hermiati *et al.*<sup>150</sup> proved that using activated carbon (1 g carbon per g biomass) as a catalyst not only increased the glucose yield during the MA-HTT of cassava pulp (32.41 to 44.49%) and tapioca flour (55.11 to 71.93% for), but also it allowed achieving the same degree of conversion using lower temperatures (from 230 to 220 °C and from 240 to 200 °C for the former and the latter feedstock, respectively).

#### 5.1.4 Other factors: solid/water ratio and microwave power.

Biomass loading (solid/water ratio) and microwave power also exert significant influences on the process. Nonetheless, their effects are less critical, and few works have addressed the impact of these parameters during the production of sugars by MA-HTT of biomass. Yuan *et al.*<sup>141</sup> revealed that a decrease in the solid/water ratio (5.63–0.63 wt% biomass loading) increased the monosaccharide yield (100–176.18 mg g<sup>-1</sup>) during the MA-HTT of brown seaweed at 150 °C with 0.4 M H<sub>2</sub>SO<sub>4</sub>. These data are in good agreement with the work of Remón *et al.*,<sup>169</sup> who found that an increase in the solid/water ratio decreased the amounts of sugars during the MA-HTT of several biomass structural components (cellulose, hemicellulose and alginic acid). Both authors reported that such an effect was accounted for by a less efficient water biomass contact when high solid/water ratios were used.

An increase in microwave power produces higher power densities, increasing production rates and diminishing associated energy production costs.<sup>130</sup> Thangavelu *et al.*<sup>138</sup> found that the highest glucose yield (43.8%) was obtained with a high microwave power (900 W) during the MA-HTT of sago pith using carbon dioxide as a catalyst. In another study, these authors also proved that an increase in the microwave power exerted a positive effect on the glucose yield using H<sub>2</sub>SO<sub>4</sub>; however, when HCl was used as a catalyst, the microwave power had a negligible effect.<sup>140</sup> Despite these positive features, an excessively high power favours the degradation of sugars in secondary products, especially if long reaction times are used. As such, the microwave power must be carefully controlled to avoid both the degradation of sugars and unnecessary energy processing costs.<sup>130</sup> Given these antagonistic influences, several authors have concluded that the best combination for glucose production consisted of high microwave powers combined with short irradiation times.<sup>33,134,140,150</sup>

## 5.2 Production of furans (furfural and 5-hydroxymethyl furfural) and carboxylic acids by MA-HTT of biomass

Furfural (pentose decomposition product) and 5-hydroxymethyl furfural (HMF, hexose decomposition product) are two of the most promising platform molecules synthesised from biomass. They can be used in various applications, including adhesives, resins, lubricants, and plastics in both the chemical and/or fuel fields.<sup>158</sup> The current methods for the productions of furfural and HMF are expensive, energy-intensive, and harmful to the environment.<sup>158</sup> Thus, greener and more energy-efficient methodologies should be developed.<sup>170–174</sup> Besides, levulinic acid (LA) is another important green platform chemical produced using biomass as a feedstock. LA derivatives are more environmentally friendly alternatives to the fossil fuel resources currently used in organic and polymer synthesis and the fuel industry.<sup>20,161</sup> Consequently, there has been a significant increase in the number of publications reporting on the production of furfural, HMF and LA from biomass.<sup>175–177</sup> Recently, particular emphasis has been placed on MA-HTT, as a rapid efficient and selective heating approach, to increase the yield of biomass dehydration products from carbohydrates and the specificity of isomerisation reactions for the production of these compounds.<sup>178</sup> The effects of the most crucial MA-HTT processing conditions reported in the literature affecting the yields and purities of these products are summarised as follows.

**5.2.1 Reaction temperature.** Temperature plays a crucial role in the production of furans from biomass carbohydrates. A relatively high temperature is required to promote saccharide dehydration reactions to furfural/HMF. However, this temperature must be controlled carefully, as excessive temperatures promote the successive transformation of furans into carboxylic acids and soluble and insoluble humins *via* rehydration and polymerisation reactions, thus decreasing the yield and selectivity of furans (HMF/furfural).<sup>179</sup> Several authors have reported on this dual effect in the literature. Ren *et al.*<sup>157</sup> produced furfural from corncob with SnCl<sub>4</sub> as a catalyst and found that the yield of furfural firstly increased with increasing temperature up to 160 °C, the temperature at which the highest furfural yield was achieved. A subsequent increase from 160 to 180 °C led to a slight decrease in the production of furfural, while a sharp drop was observed above 190 °C due to the complete degradation of furfural. Similarly, Möller *et al.*<sup>180</sup> studied the production of HMF from the decomposition of fructose. They found that the HMF yield increased (10–46%) with rising temperature (180–220 °C) until a maximum was reached. A subsequent temperature increase decreased the HMF yield (37.5%) due to its decomposition into other species. Bernal *et al.*<sup>156</sup> produced furfural from corn stover hemicelluloses *via* a two-step cascade process. These authors also indicated that the furfural yield initially increased (4.6 to 7.1 mol%) with increasing temperature (up to 190 °C). In comparison, a further increase in the temperature up to 200 °C led to a depletion in the furfural yield (5.5 mol%). Yemiş *et al.*<sup>158</sup> used the response surface methodology to opti-



mise the furfural and HMF production from wheat straw. They revealed that the pH of the solution plays the most significant role in the furfural production, with the highest furfural yield (51.3%) being obtained at 155 °C, using a reaction time of 31 min and a pH of 0.6 with 150 mL g<sup>-1</sup> biomass loading. They reported that the low acidity (pH = 0.6) of the processing solution promoted the hydrolysis of the feedstock. This study also revealed that both furfural and HMF yields displayed a linear increase with increasing temperature up to 170 °C, with the yields of these compounds diminishing as the temperature increased (above 170 °C for furfural or 180 °C for HMF). The latter also indicated that the stability of furfural was lower than that of HMF.

The production of carboxylic acids usually requires higher process severity. Aldehydes (HMF and furfural) can degrade to carboxylic acids, including levulinic, acetic and formic acids, during the MA-HTT of biomass.<sup>146</sup> Compared to their precursors, acid formation requires severer reaction conditions (higher temperatures and longer times) and the increases of acid yields correspond to the reduction of aldehydes.<sup>44</sup> There are a few works in the literature addressing the effect of the reaction time to maximise the yields and selectivity of carboxylic acids during the MA-HTT of different biomass types. Cao *et al.*<sup>80</sup> studied the production of LA from red seaweed and revealed that at a low temperature (160–180 °C), the yield of LA increased with prolonging the reaction time (1–40 min). Then, it reached a maximum value (180 °C and 200 °C with processing times of 20 and 10 min, respectively), showing that higher temperatures decrease the reaction time to achieve this value due to the significant relationship between the temperature and reaction time (process severity). Sweygers *et al.*<sup>181</sup> used cellulose, as a biomass structural compound, to optimise the MA-HTT processing conditions for LA production. They reported that at a low temperature (160 °C), the highest yield of LA (34.03 ± 0.07 wt%) was obtained after 11 min. However, when the temperature was increased up to 180 °C using the same reaction time, the yield rose to 42.96 wt%. A slightly higher LA yield (43.33 wt%) was attained by shortening the reaction time down to 1 min and increasing the temperature up to 200 °C. Antonetti *et al.*<sup>44</sup> optimised the productions of furfural and levulinic acid from giant reed by MA-HTT. These authors demonstrated that, when the process was conducted using a reaction time of 20 min, furfural was the main hydrolysis product at a relatively low temperature (up to 160 °C). At the same time, LA was the primary product when higher processing temperatures (above 160 °C) were used. As such, the production of LA was appropriate under severe reaction conditions (temperature between 170 and 190 °C). Ren *et al.*<sup>157</sup> also observed that the yields of carboxylic acids (levulinic and formic acids) presented a gradually increasing trend from 160 to 170 °C. This was followed by diminishes above 180 °C in some cases, thus confirming that carboxylic acid productions are favoured under severe processing conditions. Interestingly, the yield of acetic acid was more temperature stable than that of LA. They suggested that the breakage of acetyl groups from hemicellulose occurred from the beginning

of the reaction, thus explaining the different behaviour of both acids.

**5.2.2 Reaction time.** Reaction time is an essential factor to control the selectivity and production of furans and carboxylic acids from biomass. The application of long reaction times at low temperatures favours the formation of furans, but using prolonged reaction times at high temperatures may also promote their further decomposition (HMF dehydrogenation to carboxylic acids and/or polymerisation to humins). As such, the reaction time used during the MA-HTT of biomass must be carefully controlled to maximise the yields of the targeted products, *i.e.*, furans and/or carboxylic acids.

Hansen *et al.*<sup>179</sup> studied the conversion of fructose to HMF by MA-HTT and found that the yield of HMF linearly increased (from 17% to 33%) with prolonging the reaction time (up to 20 min) at a relatively low temperature (140 °C). However, when a higher temperature (200 °C) was used, the reaction time needed to achieve the same conversion degree was significantly shorter. For example, when the process was conducted using a reaction time as fast as 1 s, up to 52% of the fructose was converted into HMF (63% HMF yield). At the same temperature (200 °C), the effect of the reaction time was more important, and an increase from 1 to 60 s allowed an almost complete cellulose conversion to be achieved (95%). However, the HMF yield decreased (53%), thus indicating that the combination of long reaction times with high temperatures promoted not only the conversion of fructose to HMF, but also the subsequent dehydration of the HMF produced, yielding carboxylic acids (levulinic and formic acids). In another study, Ren *et al.*<sup>157</sup> also proved that high temperatures (160–180 °C) maximised the yields of furfural/HMF. The productions of these species initially increased up to a maximum with increasing reaction time. Still, they dropped when longer reaction times were used due to the formation of degradation products. They indicated that the higher the temperature, the shorter was the time needed to achieve such diminishments. These trends were confirmed by da Silva Lacerda *et al.*,<sup>154</sup> who developed kinetic models for the productions of HMF and furfural from four different lignocellulosic feedstocks. Sudipta De<sup>182</sup> studied the production of HMF from fructose in the presence of AlCl<sub>3</sub> at 120 °C. They discovered that at early reaction stages (between 30 s to 2 min), the yield of HMF increased rapidly (up to 47.8% within the first 30 s and to 52.3% in the next 90 s). However, a further increase in the reaction time up to 20 min increased the HMF yield very slowly up to 55.7%. Francavilla *et al.*<sup>161</sup> addressed the production of HMF from seaweed-derived agarose at 180 °C in the absence of a catalyst. They reported that the HMF yield increased within the first 10 min of the reaction, conditions under which a maximum was observed. Longer irradiation times (20 and 30 min) resulted in a decrease in the HMF yield.

Cao *et al.*<sup>80</sup> studied the valorisation of *Gracilaria lemaneiformis* (a red seaweed) *via* MA-HTT to produce levulinic acid (LA). They found that the yield of LA increased from 1 to 40 min when a low temperature (160 °C) was used. An increase in the reaction temperature (up to 180 and 200 °C) decreased the



time needed to achieve the same conversion degree (down to 20 and 10 min, respectively). These diminishments indicated that higher temperatures reduced the reaction time required to reach equilibrium conditions. Nevertheless, Lappalainen *et al.*<sup>160</sup> demonstrated that the reaction time must be controlled carefully. At 180 °C, the LA yield obtained at 40 min was higher than that with a 50 min processing time, due to the decomposing of LA when prolonged reaction times are used.

**5.2.3 Catalyst.** Carboxylic and mineral acids ( $\text{H}_2\text{SO}_4$ ,  $\text{HCl}$ ,  $\text{H}_3\text{PO}_4$ ,  $\text{HNO}_3$ ,  $\text{CH}_3\text{COOH}$ ,  $\text{HCOOH}$ ) and alkali salts ( $\text{MgCl}_2$ ,  $\text{AlCl}_3 \cdot 6\text{H}_2\text{O}$ ) have been used for the transformation of biomass into furans and/or carboxylic acids.<sup>182</sup> The effects of the catalyst type and loading on the MA-HTT of biomass to produce valuable liquids are described as follows.

Ren *et al.*<sup>157</sup> studied the effect of using  $\text{SnCl}_4$  as a catalyst for furfural production by MA-HTT of corncob. They reported that the catalyst promoted not only the hydrolysis of hemicelluloses effectively, but also the dehydration of pentoses to furfural. Yemiş *et al.*<sup>183</sup> compared 14 kinds of metal halides to be used as the catalyst to obtain furfural from straw biomass by MA-HTT. Among them,  $\text{FeCl}_3$  was the most efficient catalyst, with a furfural yield shifting between 35.3% and 65.3%, depending on the conditions. These authors also tested six types of acids, including strong mineral acids (hydrochloric acid, sulfuric acid, phosphoric acid and nitric acid) and weak organic acids (acetic acid and formic acid), for the conversion of xylan into furfural. Under the same processing MA-HTT conditions (180 °C, 20 min, 1:100 m/m biomass loading), the highest furfural yield (37.5%) was attained with hydrochloric acid. Shao *et al.*<sup>155</sup> studied the HMF production from sugarcane catalysed with  $\text{HCl}$  in seawater and acidic seawater, using a temperature ranging from 130 to 180 °C and a reaction time shifting between 1 and 60 min. Experimental results revealed that LA production was inhibited in seawater. They reported that alkali and alkaline earth metal chlorides ( $\text{NaCl}$ ,  $\text{CaCl}_2$ , and  $\text{MgCl}_2$ ) were responsible for inhibiting the dehydration of HMF to LA. Wu *et al.*<sup>20</sup> characterised the water-soluble products from the acid-catalysed ( $\text{H}_2\text{SO}_4$ ), MA-HTT of starch *via*  $^{13}\text{C}$  NMR spectroscopy. They reported that the liquid phase contained a higher LA amount when a low concentration of sulfuric acid was used. In contrast, an increase in the yield of a spherical solid residue was observed using higher acid concentrations. They indicated that this solid formation might be accounted for by the positive catalytic effect of  $\text{H}_2\text{SO}_4$  on the first transformation of glucose to HMF and the subsequent degradation of the latter species into humins. Cao *et al.*<sup>80</sup> studied the production of LA by MA-HTT at 180 °C from *Gracilaria lemaneiformis* using  $\text{H}_2\text{SO}_4$  as a catalyst. Their results revealed that an initial addition of acid significantly increased the yield of LA (from 4 to 15 wt%) until a point at which raising the catalyst amount resulted in a meagre catalytic effect, and the LA yield remained steady at around 17 wt%.

**5.2.4 Other factors: solid/water ratio, type of biomass and microwave power.** Da Silva Lacerda *et al.*<sup>154</sup> studied the influ-

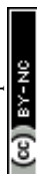
ence of biomass loading on the production of furfural and HMF during the MA-HTT of different lignocellulosic feedstocks (carnauba leaves, macauba pulp, macauba shell, and pine nutshell) at 140 °C for 30 min. They reported that the production of furanic compounds was promoted using a low biomass loading (low solid/water ratio) for all the feedstocks but macauba pulp. However, with an excessively diluted (very low solid/water ratio) solution, furan degradation took place to a substantial extent, thus increasing the presence of by-products from HMF dehydration. Yemiş *et al.*<sup>158</sup> also reported the significant effect of the biomass loading for the production of furfural by MA-HTT of wheat straw. Conversely, Cao *et al.*<sup>80</sup> reported that the yield of LA (~16%) was not affected by the biomass loading (between 1–5 wt%) at 180 °C for 40 min, while a subsequent upsurge in the biomass loading up to 10 wt% led to a decrease in the LA yield (13%).

The biomass type does also affect not only the yields of furans and carboxylic acids, but also the optimum processing conditions to achieve these optima. For example, da Silva Lacerda *et al.*<sup>154</sup> revealed that the highest HMF and furfural yields (10.01% for carnauba leaves, 15.02% for macauba shell and 15.94% for macauba pulp) were obtained under the same MA-HTT conditions (140 °C for 30 min), while for pine nutshell, the highest yield (14.98%) was obtained at 160 °C for 30 min. In this line, Antonetti *et al.*<sup>44</sup> revealed that high furfural yields were only obtained by employing a combination of fast heating and cooling systems, thus highlighting the benefits of microwave irradiation. The influence of the microwave power on the production of furans and carboxylic acids has not yet been studied in detail. Hansen *et al.*<sup>179</sup> reported that there were pronounced differences in terms of conversion or product distribution when different microwave powers (90, 150 and 300 W) were used to achieve reaction conditions (between 140 and 160 °C) using a ramp time of 5 min.

## 6. Current challenges

The data showed above clearly demonstrate that microwave-assisted hydrothermal valorisation (including all its variants, *i.e.*, MA-HTC, MA-HTL and MA-HTT) is an up-and-coming technology for the transformation of biomass into biofuels and chemicals. Despite the fact that this technology has inherent advantages over traditional hydrothermal methods using conventional heating, there are still some challenges needing further investigation.

In particular, the complex chemical reactions taking place during these valorisation processes are not yet totally understood. They need to be further investigated to provide more and new insights into the reaction mechanism. A possible approach should be the development of complex mathematical/statistical models to understand these transformations. This information might be paramount to comprehend how and to what extent the operating conditions affect the yield and composition of the reaction products. This information is vital to design large-scale reactors and improve the economics



and efficiency of this microwave-assisted technology.<sup>4,53</sup> Besides, most of the work reported to date has focused on using only one type or a few types of biomasses alone. As such, synergistic and/or antagonistic effects taking place under microwave heating when different types of biomasses are processed together have been rarely addressed. This is considered a new and interesting area of research for the development of future biorefineries.<sup>184</sup>

Besides, the efficient penetration of microwave irradiation through the feedstock is limited by the amount of biomass used in the process.<sup>185</sup> This is not an issue for lab-scale application, especially when low solid/water ratios are used; however, the ability of microwave irradiation to penetrate a large block of biomass in an industrial microwave-assisted reactor should be carefully considered.<sup>37,53,186,187</sup> The energy efficiency of a process is one of the most paramount factors determining its possible scale-up and future industrial implementation and commercialisation.<sup>42</sup> Although microwave heating can be potentially more energy-saving than conventional heating on a lab-scale,<sup>33,188,189</sup> the technology is still immature on a larger scale.

In addition, microwave heating is based on the high-frequency rotation of polar molecules, which produces quicker and higher heat of the species with high polarity.<sup>24–31</sup> Carbohydrates, including both cellulose and hemicellulose, are much polar than lignin. Consequently, they are more likely to interact with microwaves, favouring the solubilisation of the carbohydrate matter without substantially dissolving the lignin fraction.<sup>122,153</sup> Nevertheless, it is also important to note that the high crystallinity of cellulose combined with the strong hydrogen bonds within its structure hampers the depolymerisation of this carbohydrate.<sup>190,191</sup> A possible solution already adopted to overcome this issue was the addition of a homogeneous catalyst such as acetic acid, which allowed the solubilisation of cellulose and hemicellulose in lignocellulosic biomass without dissolving its lignin content.<sup>153</sup>

Given all these challenges, future work should also evaluate whether the microwave-assisted conversions are techno-economic feasible on an industrial scale and develop novel and efficient microwave reactor configurations and designs.<sup>32,53,185</sup> Also, the separation and extraction of desired aqueous products from the product reaction mixture can also be an issue on a larger scale. Lab-scale methods, including centrifugation and organic solvents, are not feasible; hence advanced separation processes should be developed.<sup>18</sup>

## 7. Conclusions

The efficient and sustainable utilisation of lignocellulosic biomass and wastes has received increasing attention over the past few years in the production of biofuels, chemicals and biomaterials. Among the different thermochemical processes developed to date, the recently developed microwave-assisted hydrothermal technology is considered an up-and-coming methodology to convert biomass into these commodities. This

process is capable of achieving an efficient, selective, controllable and cost-effective biomass valorisation, thus improving the yield and quality of the reaction products as well as reducing the processing costs. Given these promising features, this critical review has put together and analysed all the work conducted to date on the microwave-assisted hydrothermal conversion of biomass for the first time. This includes microwave-assisted hydrothermal carbonisation, liquefaction and treatment (MA-HTC, MA-HTL and MA-HTT) to transform biomass into hydrochar, bio-crude (bio-oil), and valuable liquid chemicals. Special attention has been paid to the influence of the reaction conditions on the yield and properties of these products, studying the relationships between the processing conditions and the chemical transformations involved in the processes (hydrolysis, dehydration, decarboxylation, condensation, and re-polymerisation). Besides, the recent challenges being currently faced by microwave-assisted heating have also been highlighted, and conventional and microwave-assisted technologies have been compared when data were available.

The experimental results reported in the literature using lab-scale microwave reactors have pointed out that microwave-assisted heating technologies under hydrothermal conditions, *i.e.*, MA-HTC, MA-HTL and MA-HTT, have great potential to become efficient and environmentally friendly processes for biomass valorisation. However, more research is still needed to develop, scale-up, implement, and commercialise these technologies within a biorefinery. One of the most critical challenges might be developing industrial, pressurised microwave reactors operated in either batch or continuous (flow) mode. The efficient penetration of microwave radiation must be ensured, while the continuous operation of a pressurised stream is challenging. An intermediate approach could be using a cascade of batch or continuous reactors for the scaling-up procedure to ensure efficient microwave penetration. Simultaneously, more research should be conducted on the development and design of efficient, commercial-scale magnetrons for the future development of this emerging technology. This future scale-up and commercialisation will pave the way for an efficient, selective and controllable biomass valorisation. At the same time, future work should also include the examination of the effects of processing conditions, biomass type and microwave power on the efficiency of the processes and the yields and purities of the reaction products. The critical analysis and complete understanding of all this information are vital to pave the way for the present and future development of this cutting-edge, recently developed biomass valorisation technology.

## Author contributions

The manuscript was written through the contributions of all authors. All authors have given approval to the final version of the manuscript.



## Conflicts of interest

There are no conflicts to declare.

## Acknowledgements

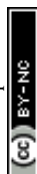
Javier Remón would like to express his gratitude to the Spanish “Ministerio de Ciencia, Innovación y Universidades” for the Juan de la Cierva Fellowship awarded (IJC2018-037110-I).

## References

- 1 K. Sipillä, E. Kuoppala, L. Fagernas and A. Oasmaa, *Biomass Bioenergy*, 1998, **14**, 103–113.
- 2 D. Sun, B. Wang, H.-M. Wang, M.-F. Li, Q. Shi, L. Zheng, S.-F. Wang, S.-J. Liu and R.-C. Sun, *ACS Sustainable Chem. Eng.*, 2018, **7**, 3073–3082.
- 3 Z. Zhang and Z. K. Zhao, *Bioresour. Technol.*, 2010, **101**, 1111–1114.
- 4 L. Cao, C. Zhang, H. Chen, D. C. Tsang, G. Luo, S. Zhang and J. Chen, *Bioresour. Technol.*, 2017, **245**, 1184–1193.
- 5 W.-H. Yan, P.-G. Duan, F. Wang and Y.-P. Xu, *Fuel*, 2016, **185**, 229–235.
- 6 L. G. Van Doren, R. Posmanik, F. A. Bicalho, J. W. Tester and D. L. Sills, *Bioresour. Technol.*, 2017, **225**, 67–74.
- 7 M. Zhou, J. Xu, J. Jiang and B. K. Sharma, *Energies*, 2018, **11**, 2877.
- 8 M. Deniel, G. Haarlemmer, A. Roubaud, E. Weiss-Hortala and J. Fages, *Energy Fuels*, 2016, **30**, 4895–4904.
- 9 S. Shukla and S. Vyas, *IOSR J. Environ. Sci., Toxicol. Food Technol.*, 2015, **9**, 37–44.
- 10 M. Kleinert and T. Barth, *Energy Fuels*, 2008, **22**, 1371–1379.
- 11 S. Kim, Y. Lee, K.-Y. A. Lin, E. Hong, E. E. Kwon and J. Lee, *J. Cleaner Prod.*, 2020, 120816.
- 12 A. Zabaniotou and P. Kamaterou, *J. Cleaner Prod.*, 2019, **211**, 1553–1566.
- 13 Z. Qin, Q. Zhuang, X. Cai, Y. He, Y. Huang, D. Jiang, E. Lin, Y. Liu, Y. Tang and M. Q. Wang, *Renewable Sustainable Energy Rev.*, 2018, **82**, 2387–2400.
- 14 J. Ren, Y.-L. Liu, X.-Y. Zhao and J.-P. Cao, *J. Energy Inst.*, 2020, **93**, 1083–1098.
- 15 H. C. Ong, W.-H. Chen, Y. Singh, Y. Y. Gan, C.-Y. Chen and P. L. Show, *Energy Convers. Manage.*, 2020, **209**, 112634.
- 16 K. Tekin, S. Karagöz and S. Bektaş, *Renewable Sustainable Energy Rev.*, 2014, **40**, 673–687.
- 17 M. Kumar, A. O. Oyedun and A. Kumar, *Renewable Sustainable Energy Rev.*, 2018, **81**, 1742–1770.
- 18 A. Kruse and N. Dahmen, *J. Supercrit. Fluids*, 2018, **134**, 114–123.
- 19 T. Wang, Y. Zhai, Y. Zhu, C. Li and G. Zeng, *Renewable Sustainable Energy Rev.*, 2018, **90**, 223–247.
- 20 D. Wu and M. Hakkarainen, *ACS Sustainable Chem. Eng.*, 2014, **2**, 2172–2181.
- 21 Z. Liu, A. Quek, S. K. Hoekman and R. Balasubramanian, *Fuel*, 2013, **103**, 943–949.
- 22 H. A. Ruiz, R. M. Rodríguez-Jasso, B. D. Fernandes, A. A. Vicente and J. A. Teixeira, *Renewable Sustainable Energy Rev.*, 2013, **21**, 35–51.
- 23 M. Kolb, H. Wichmann and U. Schröder, *Sustainable Chem. Pharm.*, 2019, **13**, 100165.
- 24 V. L. Budarin, J. H. Clark, B. A. Lanigan, P. Shuttleworth and D. J. Macquarrie, *Bioresour. Technol.*, 2010, **101**, 3776–3779.
- 25 V. L. Budarin, P. S. Shuttleworth, J. R. Dodson, A. J. Hunt, B. Lanigan, R. Marriott, K. J. Milkowski, A. J. Wilson, S. W. Breeden, J. Fan, E. H. K. Sin and J. H. Clark, *Energy Environ. Sci.*, 2011, **4**, 471–479.
- 26 M. De bruyn, J. Fan, V. L. Budarin, D. J. Macquarrie, L. D. Gomez, R. Simister, T. J. Farmer, W. D. Raverty, S. J. McQueen-Mason and J. H. Clark, *Energy Environ. Sci.*, 2016, **9**, 2571–2574.
- 27 E. M. de Melo, J. H. Clark and A. S. Matharu, *Green Chem.*, 2017, **19**, 3408–3417.
- 28 J. Fan, M. De bruyn, V. L. Budarin, M. J. Gronnow, P. S. Shuttleworth, S. Breeden, D. J. Macquarrie and J. H. Clark, *J. Am. Chem. Soc.*, 2013, **135**, 11728–11731.
- 29 J. Fan, M. De bruyn, Z. Zhu, V. Budarin, M. Gronnow, L. D. Gomez, D. Macquarrie and J. Clark, *Chem. Eng. Process.*, 2013, **71**, 37–42.
- 30 T. Li, J. Remón, Z. Jiang, V. L. Budarin and J. H. Clark, *Energy Convers. Manage.*, 2018, **155**, 147–160.
- 31 T. Li, J. Remón, P. S. Shuttleworth, Z. Jiang, J. Fan, J. H. Clark and V. L. Budarin, *Energy Convers. Manage.*, 2017, **144**, 104–113.
- 32 A. Richel and N. Jacquet, *Biomass Convers. Biorefin.*, 2015, **5**, 115–124.
- 33 E. T. Kostas, D. Beneroso and J. P. Robinson, *Renewable Sustainable Energy Rev.*, 2017, **77**, 12–27.
- 34 R. Gedye, F. Smith, K. Westaway, H. Ali and L. Baldisera, *Tetrahedron Lett.*, 1986, **27**, 279–282.
- 35 P. Priece, J. E. P. Mejia, P. D. Carà and J. A. Lopez-Sanchez, in *Sustainable Catalysis for Biorefineries*, 2018, pp. 243–299.
- 36 Z. Ni and R. I. Masel, *J. Am. Chem. Soc.*, 2006, **128**, 12394–12395.
- 37 V. G. Gude, P. Patil, E. Martinez-Guerra, S. Deng and N. Nirmalakhandan, *Sustainable Chem. Processes*, 2013, **1**, 5.
- 38 S. Nomanbhay and M. Y. Ong, *Bioengineering*, 2017, **4**, 57.
- 39 K. Kaderides, L. Papaoikonomou, M. Serafim and A. M. Goula, *Chem. Eng. Process.*, 2019, **137**, 1–11.
- 40 Y. Zhang, P. Chen, S. Liu, P. Peng, M. Min, Y. Cheng, E. Anderson, N. Zhou, L. Fan and C. Liu, *Bioresour. Technol.*, 2017, **230**, 143–151.
- 41 J. Remón, V. L. Budarin, A. S. Matharu and J. H. Clark, *Bol. Grupo Esp. Carbón*, 2019, 8–13.
- 42 E. C. Gaudino, G. Cravotto, M. Manzoli and S. Tabasso, *Green Chem.*, 2019, **21**, 1202–1235.



- 43 S. Tsubaki, K. Oono, A. Onda, K. Yanagisawa, T. Mitani and J.-i. Azuma, *Carbohydr. Polym.*, 2016, **137**, 594–599.
- 44 C. Antonetti, E. Bonari, D. Licursi, N. Nasso o Di Nasso and A. M. Raspolli Galletti, *Molecules*, 2015, **20**, 21232–21253.
- 45 S. Tsubaki, K. Oono, A. Onda, K. Yanagisawa and J.-i. Azuma, *Bioresour. Technol.*, 2012, **123**, 703–706.
- 46 S. S. Toor, L. Rosendahl and A. Rudolf, *Energy*, 2011, **36**, 2328–2342.
- 47 P. Krammer and H. Vogel, *J. Supercrit. Fluids*, 2000, **16**, 189–206.
- 48 J. Asomaning, S. Haupt, M. Chae and D. C. Bressler, *Renewable Sustainable Energy Rev.*, 2018, **92**, 642–657.
- 49 L. Wang, Y. Chang and A. Li, *Renewable Sustainable Energy Rev.*, 2019, **108**, 423–440.
- 50 T. A. Khan, A. S. Saud, S. S. Jamari, M. H. Ab Rahim, J.-W. Park and H.-J. Kim, *Biomass Bioenergy*, 2019, **130**, 105384.
- 51 R. Sharma, K. Jasrotia, N. Singh, P. Ghosh, N. R. Sharma, J. Singh, R. Kanwar and A. Kumar, *Chem. Afr.*, 2020, **3**, 1–19.
- 52 S. Nizamuddin, H. A. Baloch, G. J. Griffin, N. M. Mubarak, A. W. Bhutto, R. Abro, S. A. Mazari and B. S. Ali, *Renewable Sustainable Energy Rev.*, 2017, **73**, 1289–1299.
- 53 Z. M. Bundhoo, *Renewable Sustainable Energy Rev.*, 2018, **82**, 1149–1177.
- 54 A. Funke and F. Ziegler, *Biofuels, Bioprod. Biorefin.*, 2010, **4**, 160–177.
- 55 S. K. Hoekman, A. Broch and C. Robbins, *Energy Fuels*, 2011, **25**, 1802–1810.
- 56 O. O. Afolabi, M. Sohail and C. Thomas, *Waste Biomass Valorization*, 2015, **6**, 147–157.
- 57 S. Nizamuddin, H. A. Baloch, M. Siddiqui, N. Mubarak, M. Tunio, A. Bhutto, A. S. Jatoti, G. Griffin and M. Srinivasan, *Rev. Environ. Sci. Bio/Technol.*, 2018, **17**, 813–837.
- 58 J. Fang, L. Zhan, Y. S. Ok and B. Gao, *J. Ind. Eng. Chem.*, 2018, **57**, 15–21.
- 59 R. Sharma, K. Jasrotia, N. Singh, P. Ghosh, N. R. Sharma, J. Singh, R. Kanwar and A. Kumar, *Chem. Afr.*, 2019, 1–19.
- 60 O. F. Cruz Jr., J. Silvestre-Albero, M. E. Casco, D. Hotza and C. R. Rambo, *Mater. Chem. Phys.*, 2018, **216**, 42–46.
- 61 A. S. Semerciöz, F. Göğüş, A. Celekli and H. Bozkurt, *J. Cleaner Prod.*, 2017, **165**, 599–610.
- 62 H. B. Sharma, A. K. Sarmah and B. Dubey, *Renewable Sustainable Energy Rev.*, 2020, **123**, 109761.
- 63 M. Möller, P. Nilges, F. Harnisch and U. Schröder, *ChemSusChem*, 2011, **4**, 566–579.
- 64 S. Nizamuddin, S. S. Qureshi, H. A. Baloch, M. T. H. Siddiqui, P. Takkalkar, N. M. Mubarak, D. K. Dumbre, G. J. Griffin, S. Madapusi and A. Tanksale, *Materials*, 2019, **12**, 403.
- 65 J.-x. Wang, S.-w. Chen, F.-y. Lai, S.-y. Liu, J.-b. Xiong, C.-f. Zhou and H.-j. Huang, *J. Supercrit. Fluids*, 2020, 104858.
- 66 K. Kang, S. Nanda, G. Sun, L. Qiu, Y. Gu, T. Zhang, M. Zhu and R. Sun, *Energy*, 2019, **186**, 115795.
- 67 Y. Shao, Y. Long, H. Wang, D. Liu, D. Shen and T. Chen, *Renewable Energy*, 2019, **135**, 1327–1334.
- 68 S. Nizamuddin, M. T. H. Siddiqui, H. A. Baloch, N. M. Mubarak, G. Griffin, S. Madapusi and A. Tanksale, *Environ. Sci. Pollut. Res.*, 2018, **25**, 17529–17539.
- 69 J. Xu, J. Zhang, J. Huang, W. He and G. Li, *Bioresour. Technol. Rep.*, 2020, **9**, 100353.
- 70 L. Dai, C. He, Y. Wang, Y. Liu, R. Ruan, Z. Yu, Y. Zhou, D. Duan, L. Fan and Y. Zhao, *Bioresour. Technol.*, 2018, **247**, 234–241.
- 71 S. Khushk, L. Zhang, A. Li, M. Irfan and X. Zhang, *Pol. J. Environ. Stud.*, 2020, **29**, 1671–1681.
- 72 Y. Gao, Y. Liu, G. Zhu, J. Xu, Q. Yuan, Y. Zhu, J. Sarma, Y. Wang, J. Wang and L. Ji, *Energy*, 2018, **165**, 662–672.
- 73 S. Kannan, Y. Gariepy and G. V. Raghavan, *Waste Manage.*, 2017, **65**, 159–168.
- 74 M. Guiotoku, C. Rambo, F. Hansel, W. Magalhaes and D. Hotza, *Mater. Lett.*, 2009, **63**, 2707–2709.
- 75 S. E. Elaigwu and G. M. Greenway, *Waste Biomass Valorization*, 2019, **10**, 1979–1987.
- 76 Y. Li, N. Tsend, T. Li, H. Liu, R. Yang, X. Gai, H. Wang and S. Shan, *Bioresour. Technol.*, 2019, **273**, 136–143.
- 77 H.-M. Liu, X.-A. Xie, M.-F. Li and R.-C. Sun, *J. Anal. Appl. Pyrolysis*, 2012, **94**, 177–183.
- 78 S. E. Elaigwu and G. M. Greenway, *Fuel Process. Technol.*, 2016, **149**, 305–312.
- 79 M. Guiotoku, C. R. Rambo and D. Hotza, *J. Therm. Anal. Calorim.*, 2014, **117**, 269–275.
- 80 L. Cao, K. Iris, D.-W. Cho, D. Wang, D. C. Tsang, S. Zhang, S. Ding, L. Wang and Y. S. Ok, *Bioresour. Technol.*, 2019, **273**, 251–258.
- 81 W.-H. Chen, S.-C. Ye and H.-K. Sheen, *Bioresour. Technol.*, 2012, **118**, 195–203.
- 82 Y. Y. Teh, K. T. Lee, W.-H. Chen, S.-C. Lin, H.-K. Sheen and I. S. Tan, *Bioresour. Technol.*, 2017, **246**, 20–27.
- 83 V. Knappe, S. Paczkowski, J. Tejada, L. A. D. Robles, A. Gonzales and S. Pelz, *J. Anal. Appl. Pyrolysis*, 2018, **134**, 162–166.
- 84 S. E. Elaigwu and G. M. Greenway, *J. Anal. Appl. Pyrolysis*, 2016, **118**, 1–8.
- 85 S. Ahmad, X. Zhu, J. Luo, M. Shen, S. Zhou and S. Zhang, *Sci. Total Environ.*, 2019, **687**, 1381–1388.
- 86 S. Nizamuddin, N. Mubarak, M. Tiripathi, N. Jayakumar, J. Sahu and P. Ganesan, *Fuel*, 2016, **163**, 88–97.
- 87 K. Jacobson, K. C. Maheria and A. K. Dalai, *Renewable Sustainable Energy Rev.*, 2013, **23**, 91–106.
- 88 W.-C. Wang, Development of a Small Scale Continuous Hydrolysis Process for Drop-In Biofuel Production. Diss. North Carolina State University, 2011.
- 89 H. Kang, L. Ma, S. Zhang and J. Li, *IOP Conf. Ser.: Mater. Sci. Eng.*, 2015, **87**, 12028.
- 90 S. Kang, X. Li, J. Fan and J. Chang, *Ind. Eng. Chem. Res.*, 2012, **51**, 9023–9031.
- 91 D. T. Chadwick, K. P. McDonnell, L. P. Brennan, C. C. Fagan and C. D. Everard, *Renewable Sustainable Energy Rev.*, 2014, **30**, 672–681.



- 92 S. K. Satpathy, L. G. Tabil, V. Meda, S. N. Naik and R. Prasad, *Fuel*, 2014, **124**, 269–278.
- 93 O. O. Afolabi and M. Sohail, *Water Sci. Technol.*, 2017, **75**, 2852–2863.
- 94 L. Dai, C. He, Y. Wang, Y. Liu, Z. Yu, Y. Zhou, L. Fan, D. Duan and R. Ruan, *Energy Convers. Manage.*, 2017, **146**, 1–7.
- 95 I. Zambon, F. Colosimo, D. Monarca, M. Cecchini, F. Gallucci, A. R. Proto, R. Lord and A. Colantoni, *Energies*, 2016, **9**, 526.
- 96 N. H. Zainal, A. A. Aziz, J. Idris, R. Mamat, M. A. Hassan, E. K. Bahrin and S. Abd-Aziz, *J. Cleaner Prod.*, 2017, **142**, 2945–2949.
- 97 O. O. Afolabi, M. Sohail and C. Thomas, *Energy*, 2017, **134**, 74–89.
- 98 Y. Gao, H. Xia, A. P. Sulaeman, E. M. de Melo, T. I. Dugmore and A. S. Matharu, *ACS Sustainable Chem. Eng.*, 2019, **7**, 11861–11871.
- 99 Y. Zhang and W.-T. Chen, in *Direct Thermochemical Liquefaction for Energy Applications*, Elsevier, 2018, pp. 127–168.
- 100 V. A. Marulanda, C. D. B. Gutierrez and C. A. C. Alzate, in *Advanced Bioprocessing for Alternative Fuels, Biobased Chemicals, and Bioproducts*, Elsevier, 2019, pp. 59–81.
- 101 Y. Zhuang, J. Guo, L. Chen, D. Li, J. Liu and N. Ye, *Bioresour. Technol.*, 2012, **116**, 133–139.
- 102 S. F. K. Ahmad, M. Ali, U. Fazara, K. M. Isa, S. F. K. Ahmad, U. F. M. Ali and K. M. Isa, *Environ. Eng. Res.*, 2019, **25**, 18–28.
- 103 J. Remón, J. Randall, V. L. Budarin and J. H. Clark, *Green Chem.*, 2019, **21**, 284–299.
- 104 A. Dimitriadis and S. Bezergianni, *Renewable Sustainable Energy Rev.*, 2017, **68**, 113–125.
- 105 X.-Y. Wang, J. Leng, S.-M. Wang, A. M. Asiri, H. M. Marwani and H.-L. Qin, *Tetrahedron Lett.*, 2017, **58**, 2340–2343.
- 106 M. Grilc, G. Veryasov, B. Likozar, A. Jesih and J. Levec, *Appl. Catal., B*, 2015, **163**, 467–477.
- 107 G. Veryasov, M. Grilc, B. Likozar and A. Jesih, *Catal. Commun.*, 2014, **46**, 183–186.
- 108 M. Grilc, B. Likozar and J. Levec, *Biomass Bioenergy*, 2014, **63**, 300–312.
- 109 C. Muangsuwan, W. Kriprasertkul, S. Ratchahat, C.-G. Liu, P. Posoknistakul, N. Laosiripojana and C. Sakdaronnarong, *ACS Omega*, 2021, **6**, 2999–3016.
- 110 J. Feng, C. Hse, Z. Yang, K. Wang, J. Jiang and J. Xu, *Bioresour. Technol.*, 2017, **244**, 496–508.
- 111 A. Kržan and M. Kunaver, *J. Appl. Polym. Sci.*, 2006, **101**, 1051–1056.
- 112 H. Shao, H. Zhao, J. Xie, J. Qi and T. F. Shupe, *Int. J. Polym. Sci.*, 2019, **2019**, 7231263.
- 113 Y. Li, B. Li, F. Du, Y. Wang, L. Pan and D. Chen, *J. Appl. Polym. Sci.*, 2017, **134**, 44510.
- 114 J. Feng, J. Jiang, C.-y. Hse, Z. Yang, K. Wang, J. Ye and J. Xu, *Sustainable Energy Fuels*, 2018, **2**, 1035–1047.
- 115 C. Liu, Q. Zhao, Y. Lin, Y. Hu, H. Wang and G. Zhang, *Energy Fuels*, 2018, **32**, 510–516.
- 116 J. Xie, C.-Y. Hse, T. F. Shupe and T. Hu, *Eur. J. Wood Wood Prod.*, 2016, **74**, 249–254.
- 117 X. Zhang, K. Wu and Q. Yuan, *Energy*, 2020, 117539.
- 118 A. Lorente, J. Remón, V. L. Budarin, P. Sánchez-Verdú, A. Moreno and J. H. Clark, *Energy Convers. Manage.*, 2019, **185**, 410–430.
- 119 J. Yang, H. Chen, Q. Liu, N. Zhou and Y. Wu, *Fuel*, 2020, **282**, 118870.
- 120 A. Gollakota, N. Kishore and S. Gu, *Renewable Sustainable Energy Rev.*, 2018, **81**, 1378–1392.
- 121 J. Guo, Y. Zhuang, L. Chen, J. Liu, D. Li and N. Ye, *Bioresour. Technol.*, 2012, **120**, 19–25.
- 122 L. Zhou, V. Budarin, J. Fan, R. Sloan and D. Macquarrie, *ACS Sustainable Chem. Eng.*, 2017, **5**, 3768–3774.
- 123 J. Yang, H. Niu, A. Dalai, K. Corscadden and N. Zhou, *Fuel*, 2020, **277**, 118202.
- 124 G. Li, X. Zhu, X. Zou, Q. Xiang and Y. He, *Sci. Silvae Sin.*, 2014, **50**, 115–121.
- 125 J. Yang, H. Niu, K. Corscadden and T. Astatkie, *Appl. Energy*, 2018, **228**, 1618–1628.
- 126 Y. Qu, Q. Wei, H. Li, P. Oleskowicz-Popiel, C. Huang and J. Xu, *Bioresour. Technol.*, 2014, **162**, 358–364.
- 127 N. Sato, A. T. Quitain, K. Kang, H. Daimon and K. Fujie, *Ind. Eng. Chem. Res.*, 2004, **43**, 3217–3222.
- 128 O. Yemiş and G. Mazza, *Bioresour. Technol.*, 2011, **102**, 7371–7378.
- 129 V. Lehr, M. Sarlea, L. Ott and H. Vogel, *Catal. Today*, 2007, **121**, 121–129.
- 130 S. Ethaib, R. Omar, S. M. Kamal and D. A. Biak, *J. Eng. Sci. Technol.*, 2015, **10**, 97–109.
- 131 M. Klein, O. Griess, I. N. Pulidindi, N. Perkas and A. Gedanken, *J. Environ. Manage.*, 2016, **177**, 20–25.
- 132 P. Puligundla, S.-E. Oh and C. Mok, *Carbon Lett.*, 2016, **17**, 1–10.
- 133 J. C. López-Linares, M. T. García-Cubero, S. Lucas, G. González-Benito and M. Coca, *Chem. Eng. J.*, 2019, **368**, 1045–1055.
- 134 C. Chen, D. Boldor, G. Aita and M. Walker, *Bioresour. Technol.*, 2012, **110**, 190–197.
- 135 R. Singh, K. Bhuyan, J. Banerjee, J. Muir and A. Arora, *Ind. Crops Prod.*, 2017, **102**, 65–74.
- 136 P. Biller, C. Friedman and A. B. Ross, *Bioresour. Technol.*, 2013, **136**, 188–195.
- 137 J.-K. Xu, J.-H. Chen and R.-C. Sun, *Bioresour. Technol.*, 2015, **193**, 119–127.
- 138 S. K. Thangavelu, A. S. Ahmed and F. N. Ani, *Appl. Energy*, 2014, **128**, 277–283.
- 139 C. Sasaki, A. Kiyokawa, C. Asada and Y. Nakamura, *Waste Biomass Valorization*, 2019, **10**, 599–607.
- 140 S. K. Thangavelu, T. Rajkumar, D. K. Pandi, A. S. Ahmed and F. N. Ani, *Waste Manage.*, 2019, **86**, 80–86.
- 141 Y. Yuan and D. J. Macquarrie, *ACS Sustainable Chem. Eng.*, 2015, **3**, 1359–1365.
- 142 C. Sasaki, H. Negoro, C. Asada and Y. Nakamura, *J. Mater. Cycles Waste Manage.*, 2019, **21**, 201–204.



- 143 Z. Zhu, C. A. Rezende, R. Simister, S. J. McQueen-Mason, D. J. Macquarrie, I. Polikarpov and L. D. Gomez, *Biomass Bioenergy*, 2016, **93**, 269–278.
- 144 S. Ethaib, R. Omar, S. M. Mustapa Kamal, D. R. Awang Biak, S. Syam and M. Y. Harun, *J. Wood Chem. Technol.*, 2017, **37**, 26–42.
- 145 S. Chongkhong and C. Tongurai, *Songklanakarin J. Sci. Technol.*, 2019, **41**.
- 146 G. T. Mihiretu, M. Brodin, A. F. Chimphango, K. Øyaas, B. H. Hoff and J. F. Görgens, *Bioresour. Technol.*, 2017, **241**, 669–680.
- 147 A. d. S. e Silva, W. T. de Magalhães, L. M. Moreira, M. V. P. Rocha and A. K. P. Bastos, *Algal Res.*, 2018, **35**, 178–184.
- 148 Y. Yuan, P. Zou, J. Zhou, Y. Geng, J. Fan, J. Clark, Y. Li and C. Zhang, *Carbohydr. Polym.*, 2019, **223**, 115043.
- 149 A. Deng, J. Ren, W. Wang, H. Li, Q. Lin, Y. Yan, R. Sun and G. Liu, *Ind. Crops Prod.*, 2016, **79**, 137–145.
- 150 E. Hermiati, J.-i. Azuma, S. Tsubaki, D. Mangunwidjaja, T. C. Sunarti, O. Suparno and B. Prasetya, *Carbohydr. Polym.*, 2012, **87**, 939–942.
- 151 J. Bian, P. Peng, F. Peng, X. Xiao, F. Xu and R.-C. Sun, *Food Chem.*, 2014, **156**, 7–13.
- 152 J. Remón, T. Li, C. J. Chuck, A. S. Matharu and J. H. Clark, *ACS Sustainable Chem. Eng.*, 2019, **7**, 16160–16172.
- 153 J. Remón, A. S. Matharu and J. H. Clark, *Energy Convers. Manage.*, 2018, **165**, 634–648.
- 154 V. da Silva Lacerda, J. B. López-Sotelo, A. Correa-Guimarães, S. Hernández-Navarro, M. Sánchez-Bascones, L. M. Navas-Gracia, P. Martín-Ramos, E. Pérez-Lebeña and J. Martín-Gil, *Bioresour. Technol.*, 2015, **180**, 88–96.
- 155 Y. Shao, D. C. Tsang, D. Shen, Y. Zhou, Z. Jin, D. Zhou, W. Lu and Y. Long, *Environ. Res.*, 2020, 109340.
- 156 H. G. Bernal, L. Bernazzani and A. M. R. Galletti, *Green Chem.*, 2014, **16**, 3734–3740.
- 157 J. Ren, W. Wang, Y. Yan, A. Deng, Q. Chen and L. Zhao, *Cellulose*, 2016, **23**, 1649–1661.
- 158 O. Yemiş and G. Mazza, *Bioresour. Technol.*, 2012, **109**, 215–223.
- 159 E. S. Kim, S. Liu, M. M. Abu-Omar and N. S. Mosier, *Energy Fuels*, 2012, **26**, 1298–1304.
- 160 K. Lappalainen, N. Vogeler, J. Kärkkäinen, Y. Dong, M. Niemelä, A. Rusanen, A. L. Ruotsalainen, P. Wäli, A. Markkola and U. Lassi, *Biomass Convers. Biorefin.*, 2018, **8**, 965–970.
- 161 M. Francavilla, S. Intini, L. Luchetti and R. Luque, *Green Chem.*, 2016, **18**, 5971–5977.
- 162 S. S. Hassan, G. A. Williams and A. K. Jaiswal, *Bioresour. Technol.*, 2018, **262**, 310–318.
- 163 H. Ooshima, K. Aso, Y. Harano and T. Yamamoto, *Biotechnol. Lett.*, 1984, **6**, 289–294.
- 164 S. Vieira, M. V. Barros, A. C. N. Sydney, C. M. Piekarski, A. C. de Francisco, L. P. de Souza Vandenberghe and E. B. Sydney, *Bioresour. Technol.*, 2020, **299**, 122635.
- 165 A. Arora, P. Nandal, J. Singh and M. L. Verma, *Materials Science for Energy Technologies*, 2020, **3**, 308–318.
- 166 J. Xu, B. Liu, H. Hou and J. Hu, *Bioresour. Technol.*, 2017, **234**, 406–414.
- 167 Y. Luo, J. Fan, V. L. Budarin, C. Hu and J. H. Clark, *Green Chem.*, 2017, **19**, 4889–4899.
- 168 B. Sun, L. Duan, G. Peng, X. Li and A. Xu, *Bioresour. Technol.*, 2015, **192**, 253–256.
- 169 J. Remón, F. Santomauro, C. J. Chuck, A. S. Matharu and J. H. Clark, *Green Chem.*, 2018, **20**, 4507–4520.
- 170 F. Menegazzo, E. Ghedini and M. Signoretto, *Molecules*, 2018, **23**, 2201.
- 171 T.-W. Tzeng, P. Bhaumik and P.-W. Chung, *Mol. Catal.*, 2019, **479**, 110627.
- 172 K. Kawamura, K. Sako, T. Ogata and K. Tanabe, *Bioresour. Technol. Rep.*, 2020, **11**, 100478.
- 173 G. R. Gomes and J. C. Pastre, *Sustainable Energy Fuels*, 2020, **4**, 1891–1898.
- 174 L. Zhang, G. Xi, K. Yu, H. Yu and X. Wang, *Ind. Crops Prod.*, 2017, **98**, 68–75.
- 175 S. Dutta, K. Iris, D. C. Tsang, Z. Su, C. Hu, K. C. Wu, A. C. Yip, Y. S. Ok and C. S. Poon, *Bioresour. Technol.*, 2020, **298**, 122544.
- 176 Q. Qing, Q. Guo, P. Wang, H. Qian, X. Gao and Y. Zhang, *Bioresour. Technol.*, 2018, **260**, 150–156.
- 177 L. M. Schmidt, L. D. Mthembu, P. Reddy, N. Deenadayalu, M. Kaltschmitt and I. Smirnova, *Ind. Crops Prod.*, 2017, **99**, 172–178.
- 178 R. Weingarten, J. Cho, W. C. Conner Jr. and G. W. Huber, *Green Chem.*, 2010, **12**, 1423–1429.
- 179 T. S. Hansen, J. M. Woodley and A. Riisager, *Carbohydr. Res.*, 2009, **344**, 2568–2572.
- 180 M. Möller, F. Harnisch and U. Schröder, *Biomass Bioenergy*, 2012, **39**, 389–398.
- 181 N. Sweyggers, R. Dewil and L. Appels, *Waste Biomass Valorization*, 2018, **9**, 343–355.
- 182 S. De, S. Dutta and B. Saha, *Green Chem.*, 2011, **13**, 2859–2868.
- 183 O. Yemiş and G. Mazza, *Waste Biomass Valorization*, 2019, **10**, 1343–1353.
- 184 J. Remón, S. H. Danby, J. H. Clark and A. S. Matharu, *ACS Sustainable Chem. Eng.*, 2020, **8**, 12493–12510.
- 185 V. G. Gude, *Resour.-Effic. Technol.*, 2015, **1**, 116–125.
- 186 V. G. Gude, P. D. Patil, S. Deng and N. Nirmalakhandan, *Green chemistry for environmental remediation*, Wiley Interscience, New York, 2011, pp. 209–249.
- 187 R. Sanghi and V. Singh, *Green chemistry for environmental remediation*, John Wiley & Sons, 2012.
- 188 P. P. Falciglia, P. Roccaro, L. Bonanno, G. De Guidi, F. G. Vagliasindi and S. Romano, *Renewable Sustainable Energy Rev.*, 2018, **95**, 147–170.
- 189 S.-H. Ho, C. Zhang, W.-H. Chen, Y. Shen and J.-S. Chang, *Bioresour. Technol.*, 2018, **264**, 7–16.
- 190 N. Mosier, C. Wyman, B. Dale, R. Elander, Y. Y. Lee, M. Holtzapple and M. Ladisch, *Bioresour. Technol.*, 2005, **96**, 673–686.
- 191 Z. Jiang, J. Yi, J. Li, T. He and C. Hu, *ChemSusChem*, 2015, **8**, 1901–1907.

